Spin-wave resonance techniques

Grégoire de Loubens

Service de Physique de l'État Condensé, CEA, CNRS, Université Paris-Saclay, France

Ferromagnetic resonance

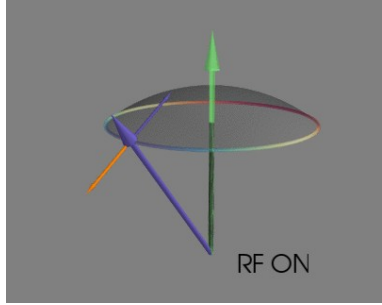

Landau-Lifshitz-Gilbert equation of motion

$$\frac{\mathrm{d}\mathbf{M}}{\mathrm{d}t} = -|\gamma|\mu_0 \mathrm{M} \times \mathbf{H_{eff}} + \alpha \frac{\mathbf{M}}{M_s} \times \frac{\mathrm{d}\mathbf{M}}{\mathrm{d}t}$$

Excitation field

$$\mathbf{h} = h_x \mathbf{u}_x + h_y \mathbf{u}_y$$

Linearization with harmonic solution

$$\mathbf{M}(t) = M_s \mathbf{u}_z + (m_x \mathbf{u}_x + m_y \mathbf{u}_y) e^{i\omega t}$$

$$\mathbf{m} = \bar{\chi}\mathbf{h} \qquad \bar{\chi} = \begin{pmatrix} \chi_{xx} & \chi_{xy} \\ \chi_{yx} & \chi_{yy} \end{pmatrix}$$

Absorbed power

$$P_{\mathrm{abs}} = \frac{1}{2}\mu_0 \omega \chi''_{xx} h_x^2$$

Kittel formula (ellipsoid)

$$\omega_0 = \gamma\mu_0 \sqrt{[H + (N_x - N_z)M_s]\,[H + (N_y - N_z)M_s]}$$

Susceptibility close to resonance $\quad \omega_0 = \gamma\mu_0 H \qquad \omega_M = \gamma\mu_0 M_s$

$$\chi'_{xx} = \chi'_{yy} = \frac{\omega_M(\omega_0 - \omega)/2}{(\omega_0 - \omega)^2 + (\alpha\omega)^2}$$

$$\chi''_{xx} = \chi''_{yy} = \frac{\omega_M(\alpha\omega)/2}{(\omega_0 - \omega)^2 + (\alpha\omega)^2}$$

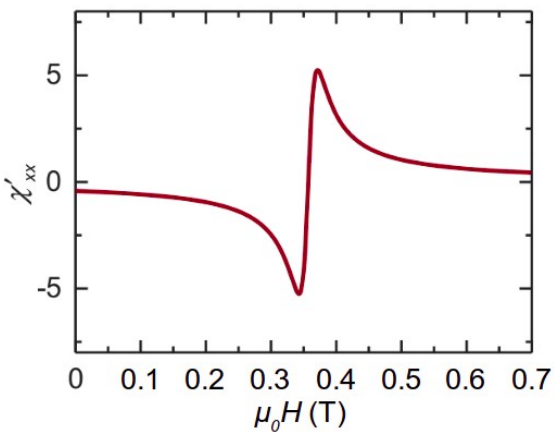

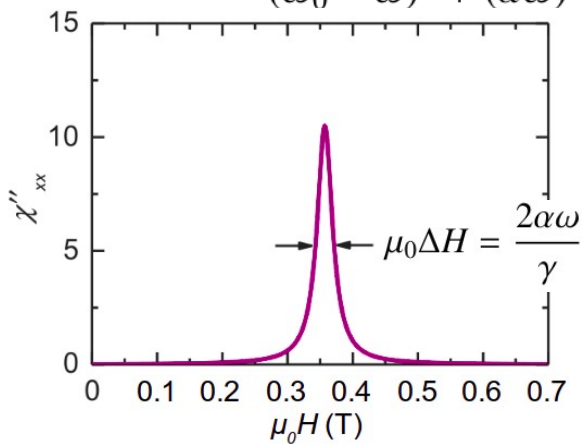

S. Rezende, *Fundamentals of Magnonics*. Springer Nature (2020)

Spin-waves in thin films

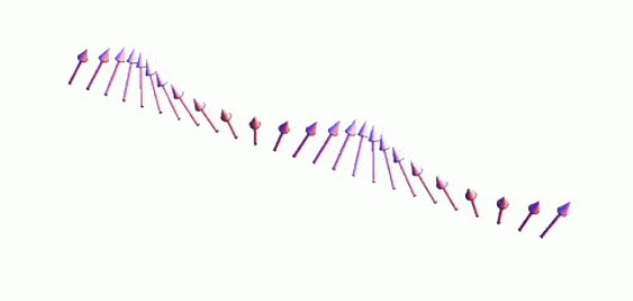

Landau-Lifshitz-Gilbert equation of motion

$$\frac{\mathrm{d}\mathbf{M}}{\mathrm{d}t} = -|\gamma|\mu_0 \mathrm{M} \times \mathbf{H_{eff}} + \alpha \frac{\mathbf{M}}{M_s} \times \frac{\mathrm{d}\mathbf{M}}{\mathrm{d}t}$$

Instantaneous magnetization distribution

$$\mathbf{M}(\mathbf{r}, t) = \mathbf{M}_{\mathrm{eq}} + \mathbf{m} e^{i(\omega t - \mathbf{k} \cdot \mathbf{r})}$$

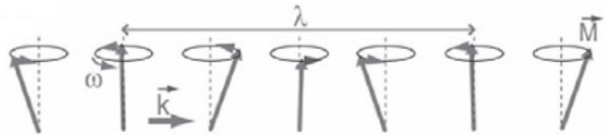

Dispersion relation

$$\omega_k = \sqrt{\left(\omega_H + \eta k_n^2\right)\left(\omega_H + \eta k_n^2 + \omega_M F_{nn}\right)}$$

$$F_{nn} = P_{nn} + \sin^2\Theta\left(1 - P_{nn}(1+\cos^2\Phi) + \omega_M \frac{P_{nn}(1-P_{nn})\sin^2\Phi}{\omega_H + \eta k_n^2}\right)$$

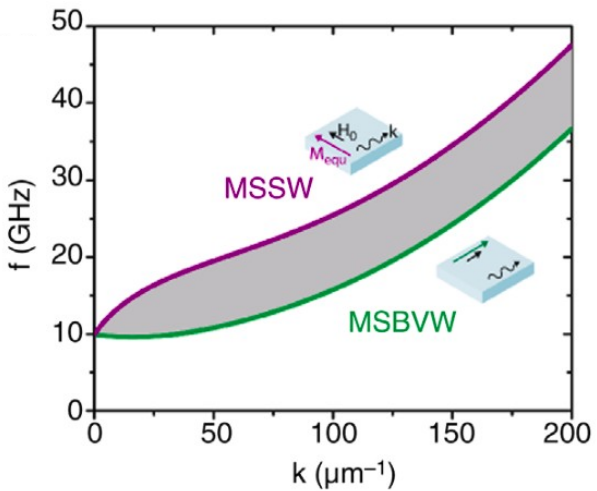

B. Kalinikos & A. Slavin, *J. Phys. C* **19**, 7013 (1986)

G. de Loubens & M. Bailleul, in *Nanomagnetism: Applications and Perspectives*. Wiley (2017)

Spin-wave eigenmodes in confined structures

Ground state

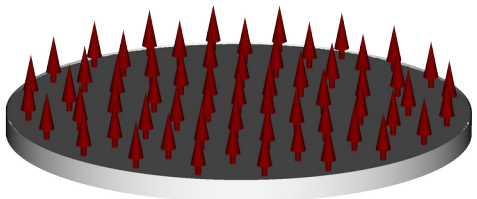

$$\frac{d\boldsymbol{M}(\boldsymbol{r})}{dt} = -|\gamma|\mu_0 \boldsymbol{M}(\boldsymbol{r}) \times \boldsymbol{H}_{\boldsymbol{eff}}(\boldsymbol{r}) + \alpha \frac{\boldsymbol{M}(\boldsymbol{r})}{M_s} \times \frac{d\boldsymbol{M}(\boldsymbol{r})}{dt}$$

$$\boldsymbol{M}(\boldsymbol{r},t)/M_s = \hat{\boldsymbol{u}}(\boldsymbol{r}) + \boldsymbol{m}(\boldsymbol{r},t) + \mathcal{O}(\boldsymbol{m}^2) \quad (|\boldsymbol{m}| \ll 1)$$

Spectroscopy

$$\omega_\nu = \frac{\langle \overline{\boldsymbol{m}_\nu} \cdot \widehat{\boldsymbol{\Omega}} * \boldsymbol{m}_\nu \rangle}{\mathcal{N}_\nu}$$ frequency

$$\Gamma_\nu = \alpha\omega_\nu \frac{\langle \overline{\boldsymbol{m}_\nu} \cdot \boldsymbol{m}_\nu \rangle}{\mathcal{N}_\nu}$$ linewidth

$$h_\nu = \frac{\langle \overline{\boldsymbol{m}_\nu} \cdot \boldsymbol{h}_1 \rangle}{\mathcal{N}_\nu}$$ amplitude

Spin-wave excitations

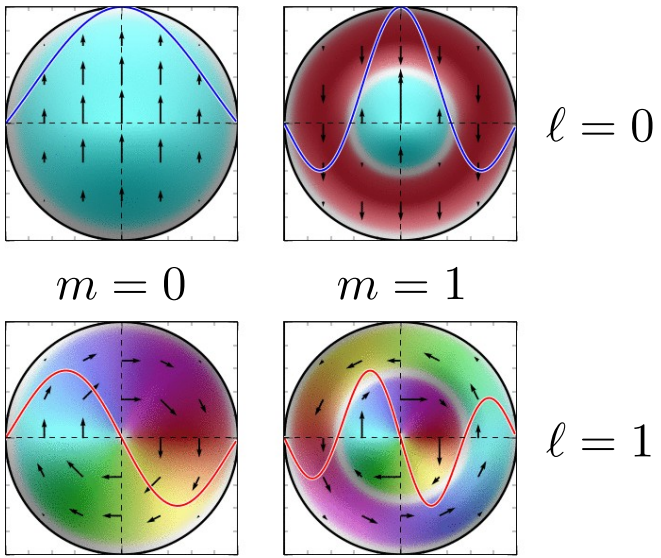

Quantized spin-wave modes in confined geometries

V. Naletov et al. *Phys. Rev. B* **84**, 224423 (2011)

Outline

- **Electrical techniques**
  - Broadband and cavity ferromagnetic resonance
  - Propagating spin-wave spectroscopy
  - Magneto-resistive detection of spin-waves
- **Optical techniques**
  - Time-resolved magneto-optical Kerr effect
  - Time-resolved X-ray imaging
  - Brillouin light scattering
- **Scanning probe techniques**
  - Magnetic resonance force microscopy
  - NV magnetometry

Outline

- **Electrical techniques**
  - Broadband and cavity ferromagnetic resonance
  - Propagating spin-wave spectroscopy
  - Magneto-resistive detection of spin-waves
- **Optical techniques**
  - Time-resolved magneto-optical Kerr effect
  - Time-resolved X-ray imaging
  - Brillouin light scattering
- **Scanning probe techniques**
  - Magnetic resonance force microscopy
  - NV magnetometry

Inductive detection of magnetic resonance

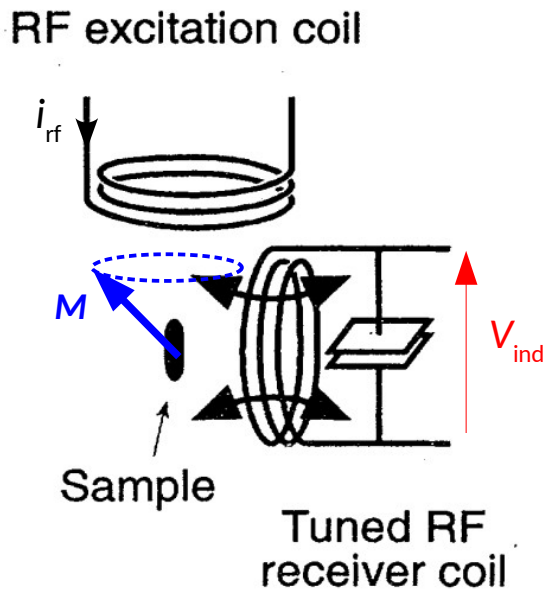

- Excitation: $i_{rf} \rightarrow h_{rf} \rightarrow dM/dt$
- Detection: $dM/dt \rightarrow V_{ind}$
- Inductive signal proportional to magnetization, volume and frequency

Broadband ferromagnetic resonance of thin films

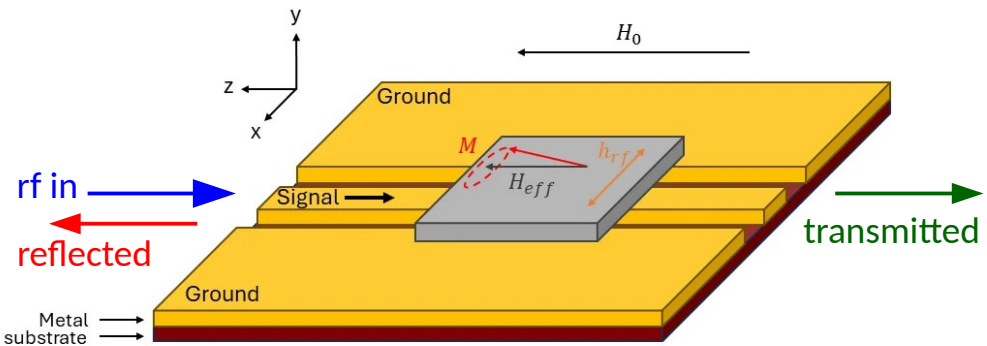

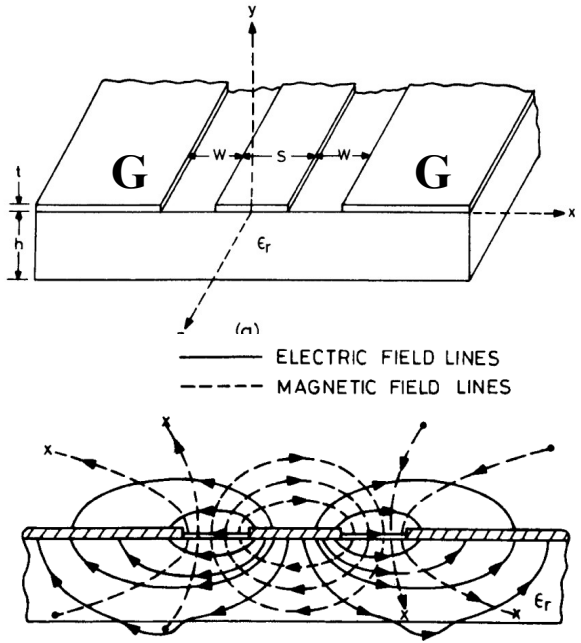

$$P_{\text{abs}} = \frac{1}{2}\mu_0 \omega \chi''_{xx} h_x^2$$

Absorbed power at FMR
→ changes in transmitted and reflected powers

K. C. Gupta et al. *Microstrip Lines and Slotlines*, Artech House (1996)

Measurement approaches

Field-differential power detection (diode)

Vector Network Analyzer

Field-differential phase-resolved microwave magnetic spectroscopy

W. Legrand et al. *Rev. Sci. Instrum.* **96**, 034708 (2025)

Extraction of magnetic parameters using broadband FMR

f = 9 GHz

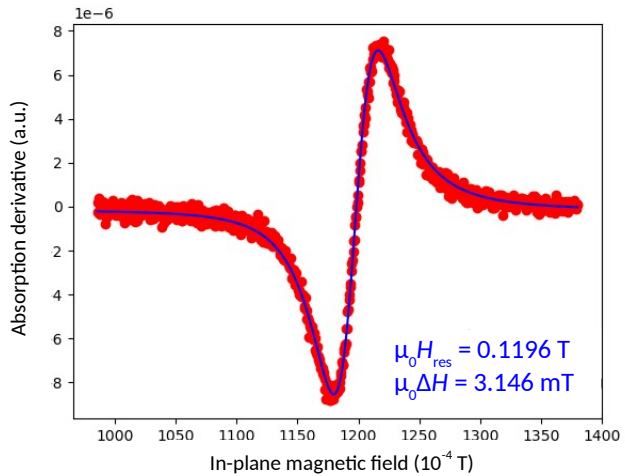

Field modulation → diode signal = dP_{abs}/dH

→ signal = Lorentzian derivative

$$\Delta H = \Delta H_{pp} \times \sqrt{3}$$

Si/SiO_2/Ta/MgO/CoFeB 1.5 nm/Ta 0.2 nm/CoFeB 1 nm/MgO/Ta

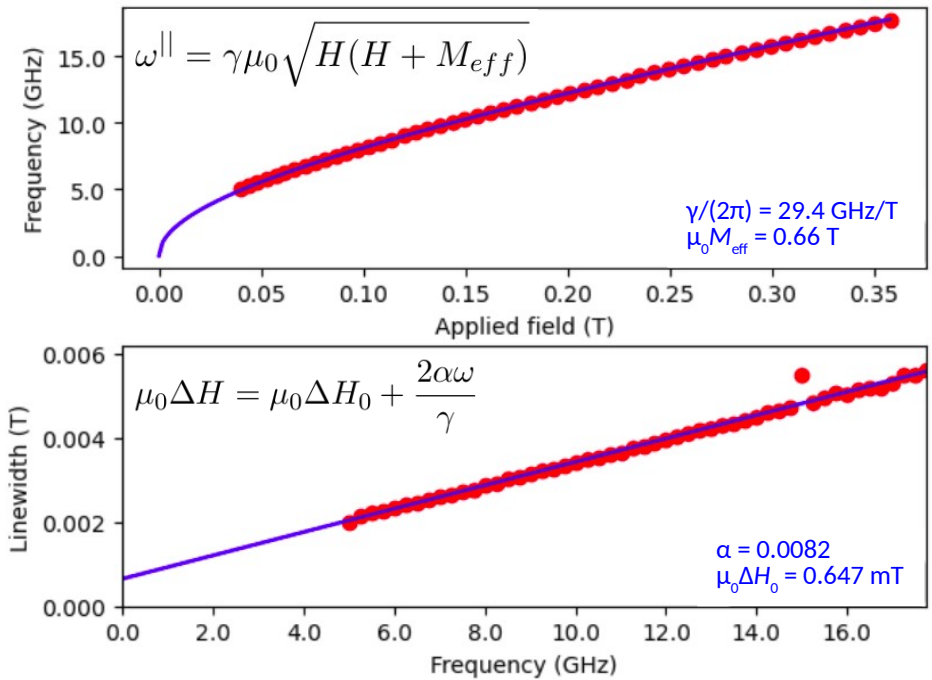

$$M_{eff} = M_s - H_u$$

$$H_u = \frac{2K_u}{\mu_0 M_s}$$

Measurement approaches

Field-differential power detection (diode)

Vector Network Analyzer

Field-differential phase-resolved microwave magnetic spectroscopy

W. Legrand et al. *Rev. Sci. Instrum.* **96**, 034708 (2025)

Broadband VNA-FMR of ultra-thin magnetic films

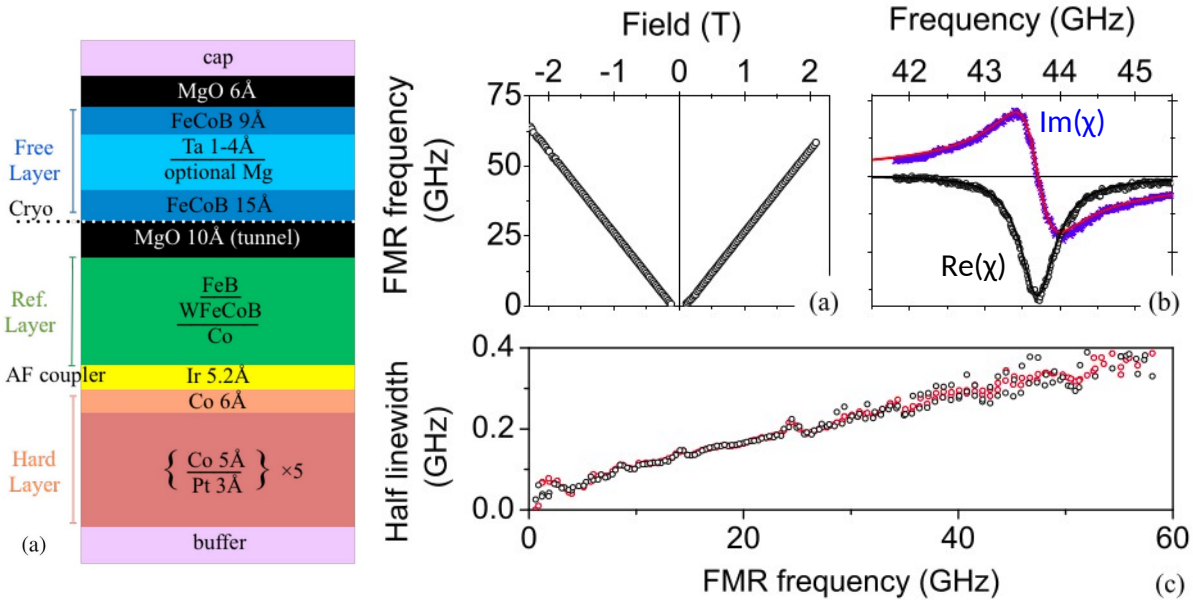

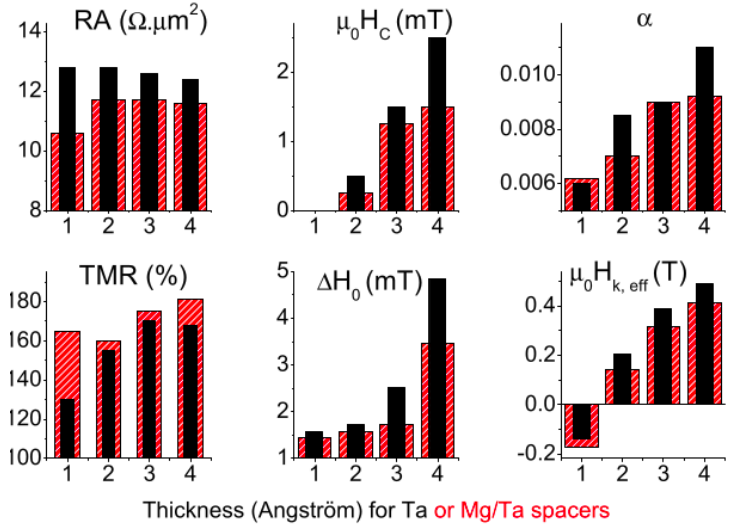

Direct access to the susceptibility in the frequency domain

T. Devolder et al. *IEEE Magn. Lett.* **10**, 5505804 (2019)

Broadband VNA-FMR of skyrmion lattice

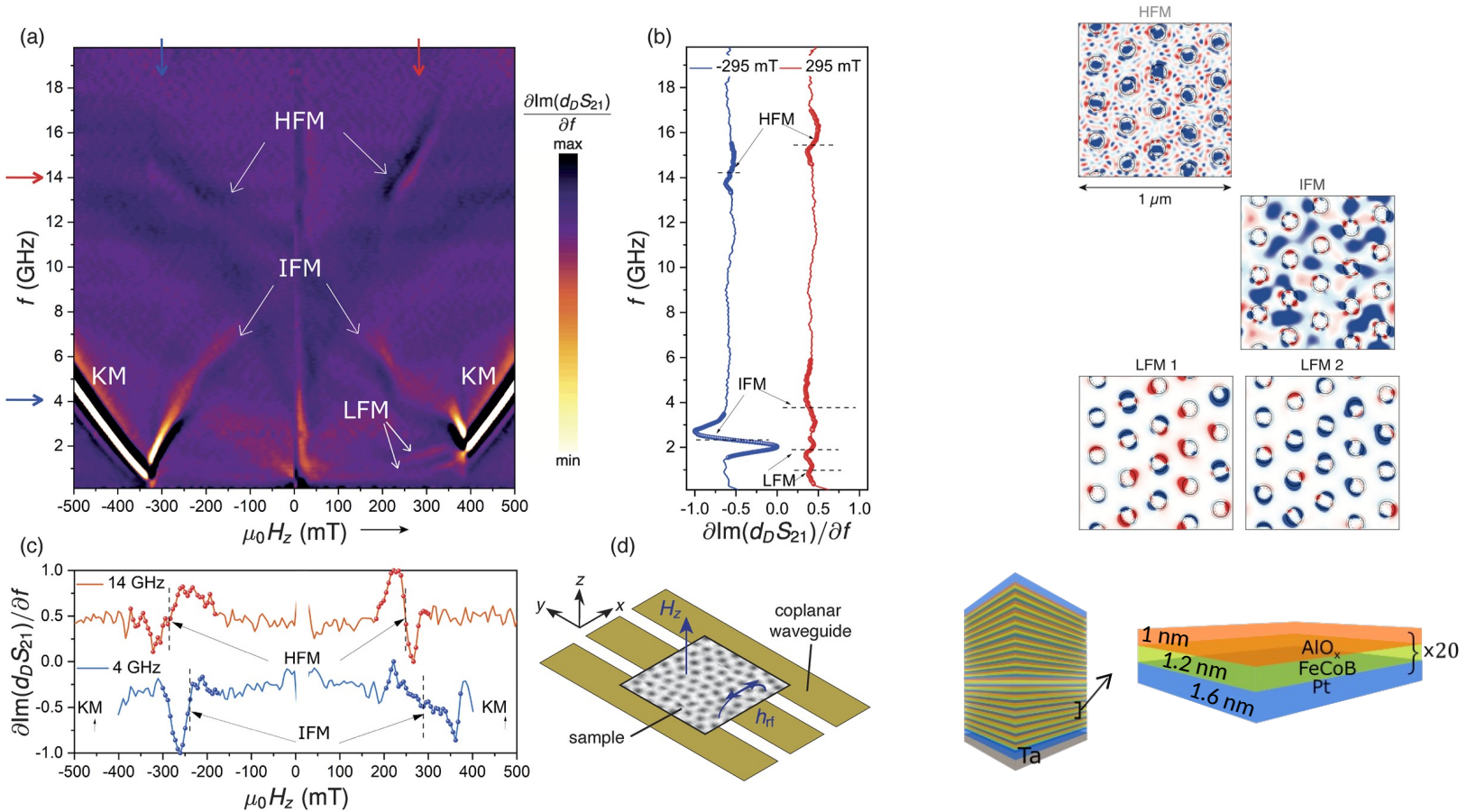

T. Srivastava et al. *APL Materials* **11**, 061110 (2023)

Cavity ferromagnetic resonance

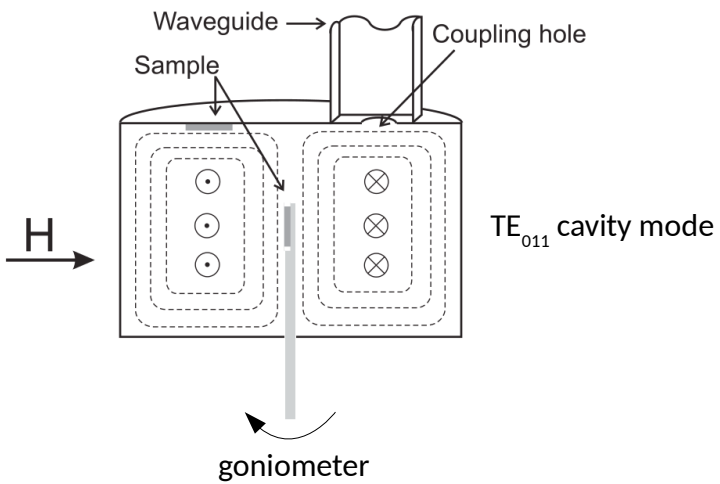

TE_{011} cavity mode

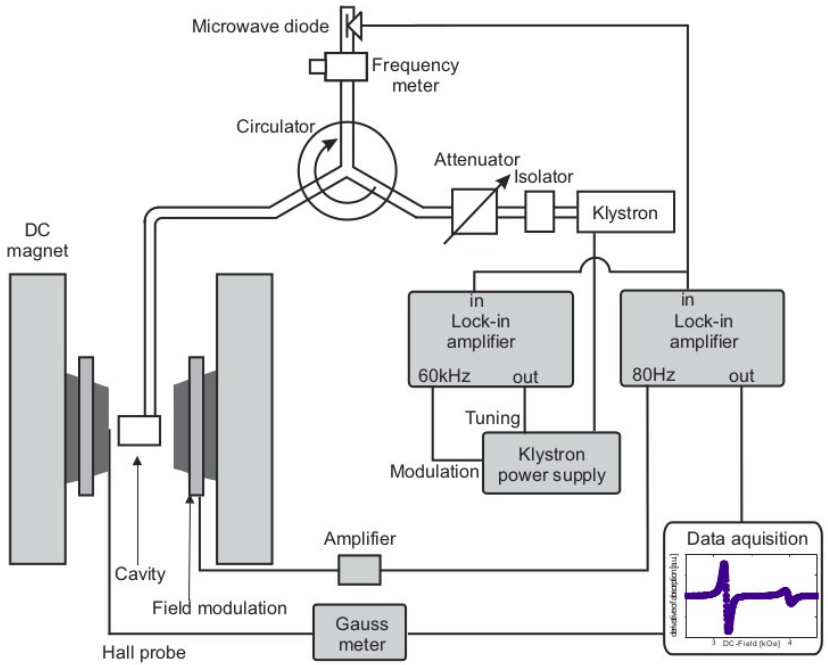

$$\text{Signal} = \frac{2\delta H V_R \beta_0^2 Q_{\text{ext}} \kappa}{(\beta_0+1)^2} \frac{\partial \chi''}{\partial H}$$

Coupling coefficient

$$\frac{1}{\beta_0} = \frac{Q_{\text{ext}}}{Q_{\text{wall}}}$$

Filling factor

$$\kappa = \frac{\Delta S t_F \langle h_{\max}^2 \rangle}{\frac{1}{8\pi}\int_{cav} \langle h(\mathbf{r})^2 \rangle d^3 r}$$

G. Woltersdorf, *PhD* thesis (2004)

Temperature and angular dependence of ferromagnetic resonance

Magnetic energy density

$$F = -MH\left[\sin\vartheta_H \sin\vartheta_M \cos(\varphi_H - \varphi_M) + \cos\vartheta_H \cos\vartheta_M\right] + K_U^* \sin^2\vartheta_M + K_1\left[\frac{1}{3}\cos^4\vartheta_M + \frac{1}{4}\sin^4\vartheta_M - \frac{\sqrt{2}}{3}\sin^3\vartheta_M \cos\vartheta_M \sin 3\varphi_M\right]$$

$$K_U^* = K_U - 2\pi M_S^2$$

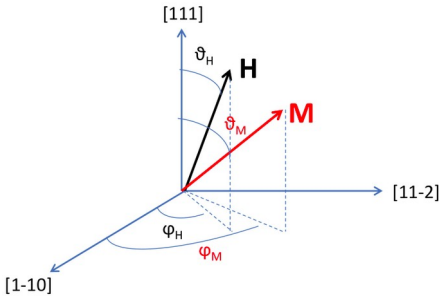

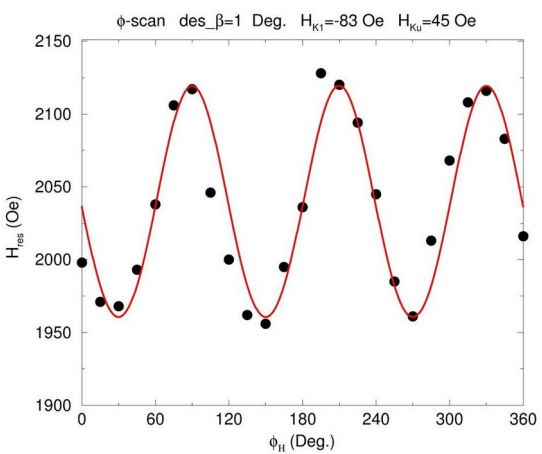

Smit & Beljers resonance condition

$$\left(\frac{\omega}{\gamma}\right)^2 = \frac{1}{M_S^2 \sin^2\vartheta_M} \times \left(\frac{\partial^2 F}{\partial\vartheta_M^2}\frac{\partial^2 F}{\partial\varphi_M^2} - \left(\frac{\partial^2 F}{\partial\vartheta_M \partial\varphi_M}\right)^2\right)$$

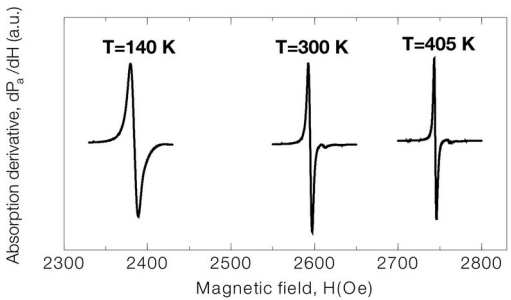

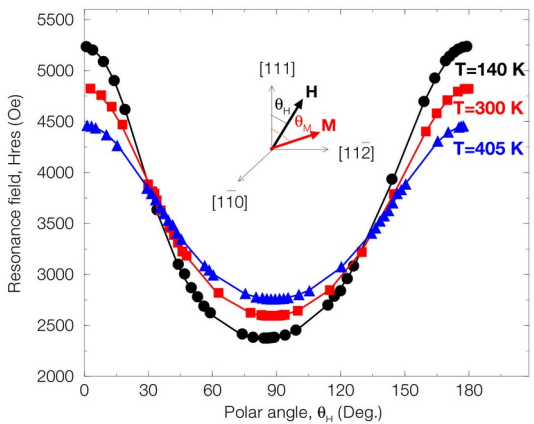

f = 9.3 GHz; GGG(111)/YIG 18 nm[/Pt 3nm]

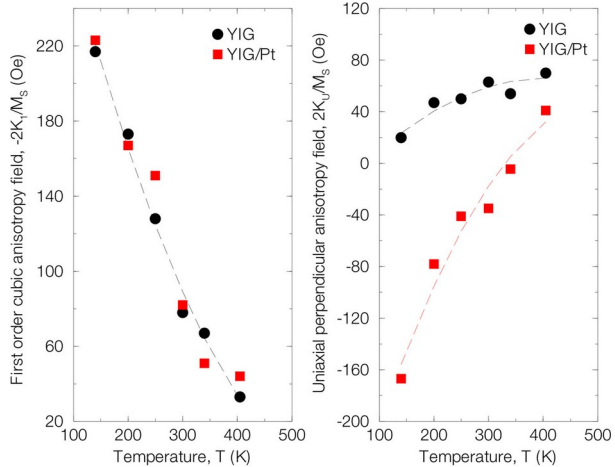

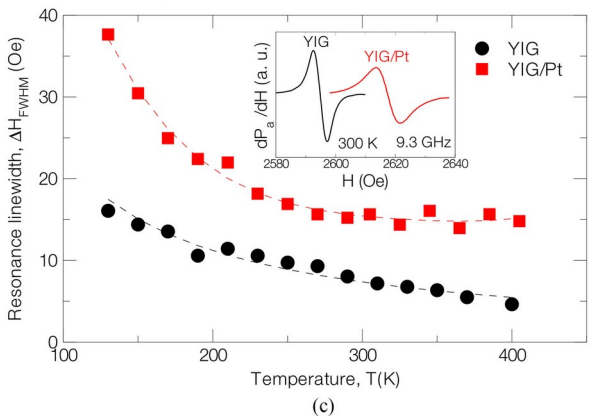

N. Beaulieu et al. *IEEE Magn. Lett.* **9**, 3706005 (2018)

Outline

- **Electrical techniques**
  - Broadband and cavity ferromagnetic resonance
  - Propagating spin-wave spectroscopy
  - Magneto-resistive detection of spin-waves
- **Optical techniques**
  - Time-resolved magneto-optical Kerr effect
  - Time-resolved X-ray imaging
  - Brillouin light scattering
- **Scanning probe techniques**
  - Magnetic resonance force microscopy
  - NV magnetometry

Propagating spin-wave spectroscopy (PSWS)

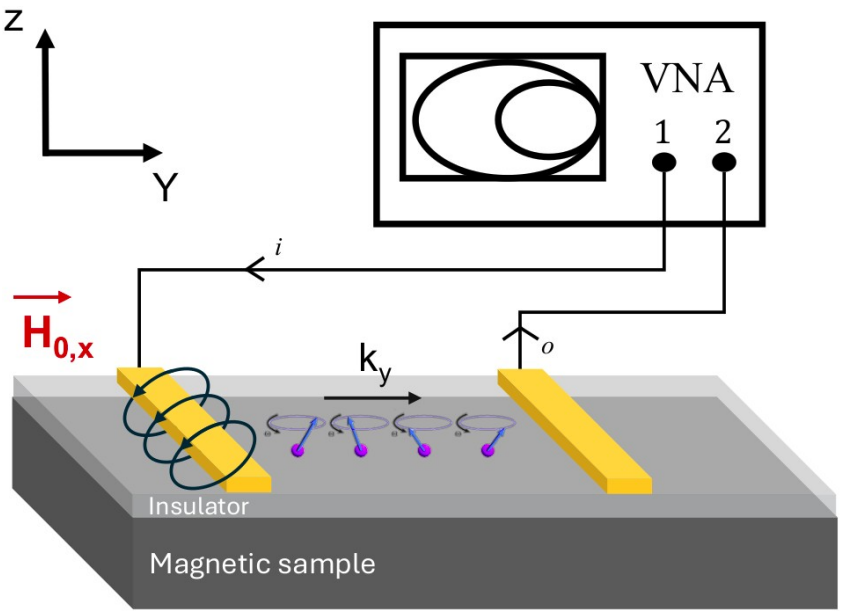

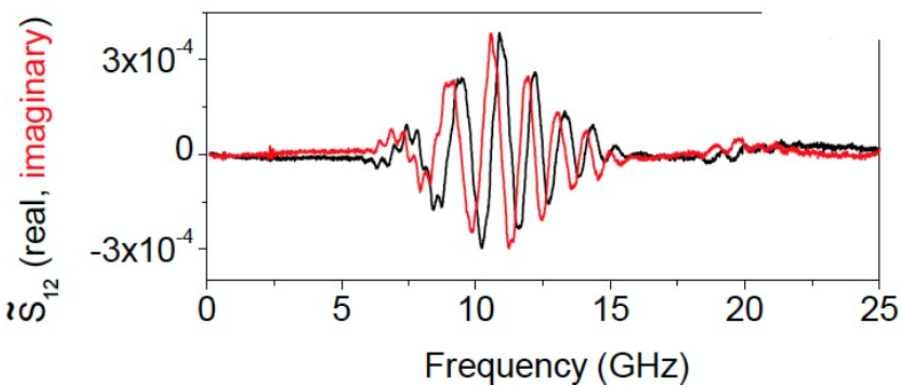

Typical spectrum in transmission: plenty information, but what exactly ?

V. Vlaminck & M. Bailleul, *Phys. Rev. B* **81**, 014425 (2010)
T. Devolder, *Phys. Rev. Appl.* **20**, 054057 (2023)

Antenna efficiency function

U-shaped antenna

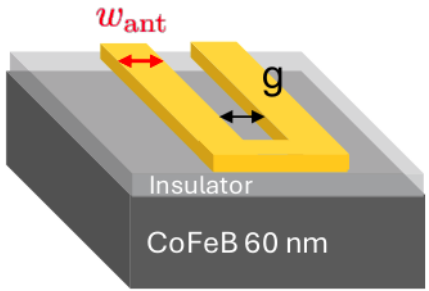

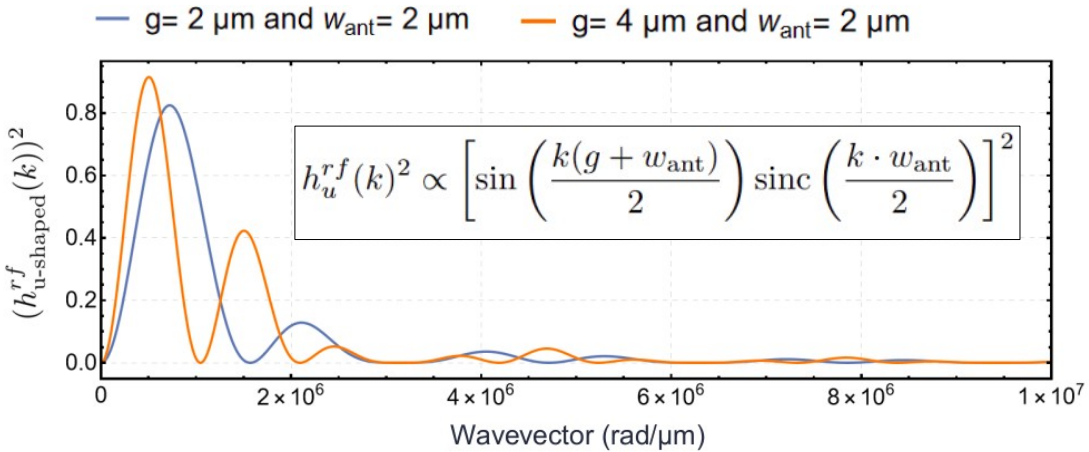

Various antennas to engineer the wavevector content

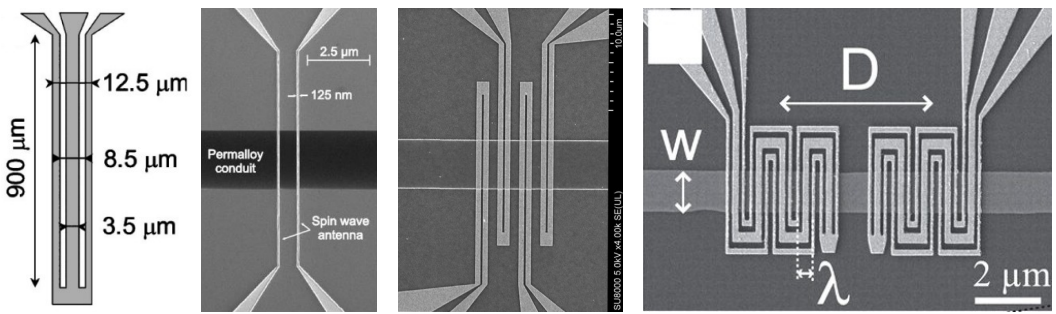

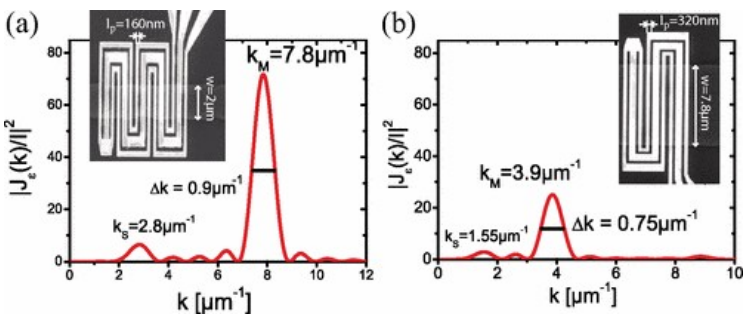

Model of spin-wave spectrum $S_{21}(\omega)$

(1) The excitation

$$h^{rf}_{\text{u-shaped}}(k) \propto \sin\left(\frac{k(g+w_{\text{ant}})}{2}\right)\text{sinc}\left(\frac{k\cdot w_{\text{ant}}}{2}\right)$$

(2) The coupling between rf-field and magnetization

$\bar{\chi}(\omega,k)$ The magnetic susceptibility tensor

$$\boldsymbol{\chi}(\omega) = \frac{\omega_M}{\omega_k^2-\omega^2+i\omega\Delta\omega_k}\cdot\begin{pmatrix}\omega_0 & i\omega & 0\\ -i\omega & \omega_k^2/\omega_0 & 0\\ 0 & 0 & 0\end{pmatrix}$$

General expression of the transmission parameter:

$$\tilde{S}_{21f}(\omega,r) \propto \frac{1}{m}\int_{\infty}[\bar{h}^*\cdot[\bar{\bar{\chi}}(\omega,k,m)\cdot\bar{h}]]e^{-ikr}(h_u^{rf}(k))^2dk$$

Detection (stray field) — Excitation field — Antenna efficiency

(3) Spin waves propagation over a distance r

e^{-ikr}

(4) The detection

Electromotive force

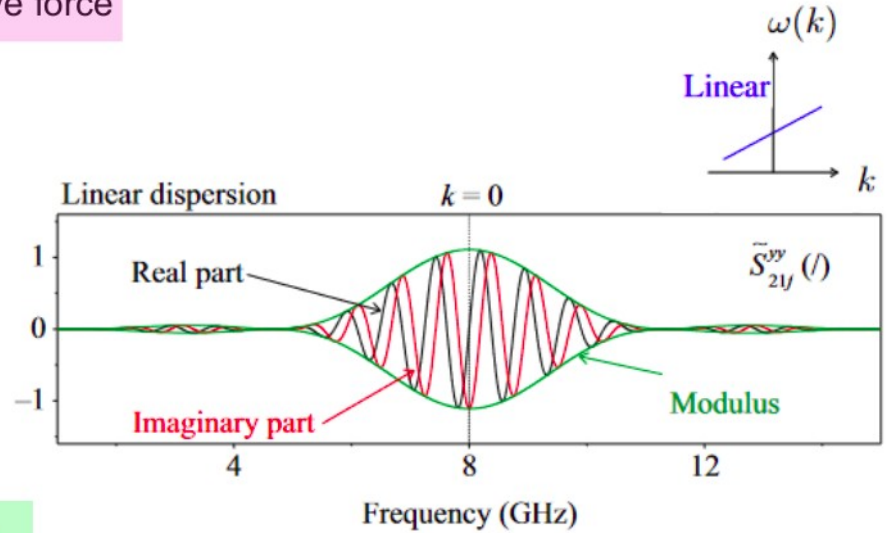

T. Devolder, *Phys. Rev. Appl.* **20**, 054057 (2023)

Model of spin-wave spectrum $S_{21}(\omega)$

(1) The excitation

$$h^{rf}_{\text{u-shaped}}(k) \propto \sin\left(\frac{k(g+w_{\text{ant}})}{2}\right)\text{sinc}\left(\frac{k\cdot w_{\text{ant}}}{2}\right)$$

(2) The coupling between rf-field and magnetization

$\bar{\chi}(\omega,k)$ The magnetic susceptibility tensor

$$\boldsymbol{\chi}(\omega) = \frac{\omega_M}{\omega_k^2-\omega^2+i\omega\Delta\omega_k}\cdot\begin{pmatrix}\omega_0 & i\omega & 0\\ -i\omega & \omega_k^2/\omega_0 & 0\\ 0 & 0 & 0\end{pmatrix}$$

General expression of the transmission parameter:

$$\tilde{S}_{21f}(\omega,r) \propto \frac{1}{m}\int_{\infty}[\bar{h}^*\cdot[\bar{\bar{\chi}}(\omega,k,m)\cdot\bar{h}]]e^{-ikr}(h_u^{rf}(k))^2dk$$

Detection (stray field) — Excitation field — Antenna efficiency

(3) Spin waves propagation over a distance r

e^{-ikr}

(4) The detection

Electromotive force

S_{21} at given frequency

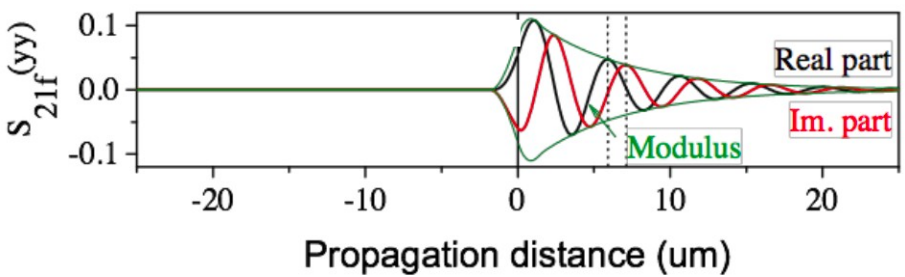

T. Devolder, *Phys. Rev. Appl.* **20**, 054057 (2023)

Attenuation length, group velocity and dispersion relation (single mode)

$$\tilde{S}_{ij}^{\text{single mode}}(\omega) \propto e^{-ik_x|r|}\, e^{-\frac{|r|}{L_{\text{att}}}}\, (h_x(k_x))^2$$

The attenuation length can be estimated from the decay of the signal between the two antennas: $2|S_{21}|/|S_{11}|$

$$L_{\text{att}} = v_g \tau$$

$\tau \simeq 1/(\alpha\omega)$ is the relaxation time

$v_g = (\partial\omega/\partial k_x)$ is the group velocity

The group velocity can be estimated from the period f_p of the oscillations of S_{21} and the distance D between antennas

$$v_g = f_p \cdot D$$

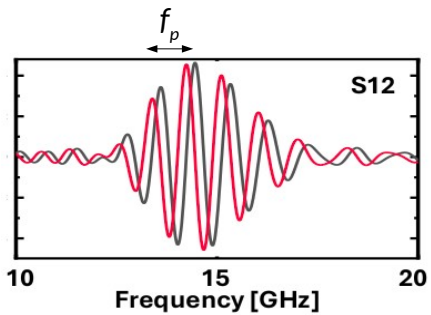

The dispersion relation of the spin-wave mode can be obtained by unwrapping of the phase

$$\frac{\tilde{S}_{ij}}{||\tilde{S}_{ij}||} = e^{-ik_x|r|} \rightarrow k_x(\omega) = -\frac{1}{r}\left[\text{Arg}\frac{\tilde{S}_{ij}(\omega)}{||\tilde{S}_{ij}(\omega)||}\right] + \frac{2n\pi}{r},\ n \in \mathbb{N}$$

V. Vlaminck & M. Bailleul, *Phys. Rev. B* **81**, 014425 (2010)
T. Devolder et al. *Phys. Rev. B* **103**, 214431 (2021)

Dispersion relations from time-of-flight spectroscopy (multi-modes)

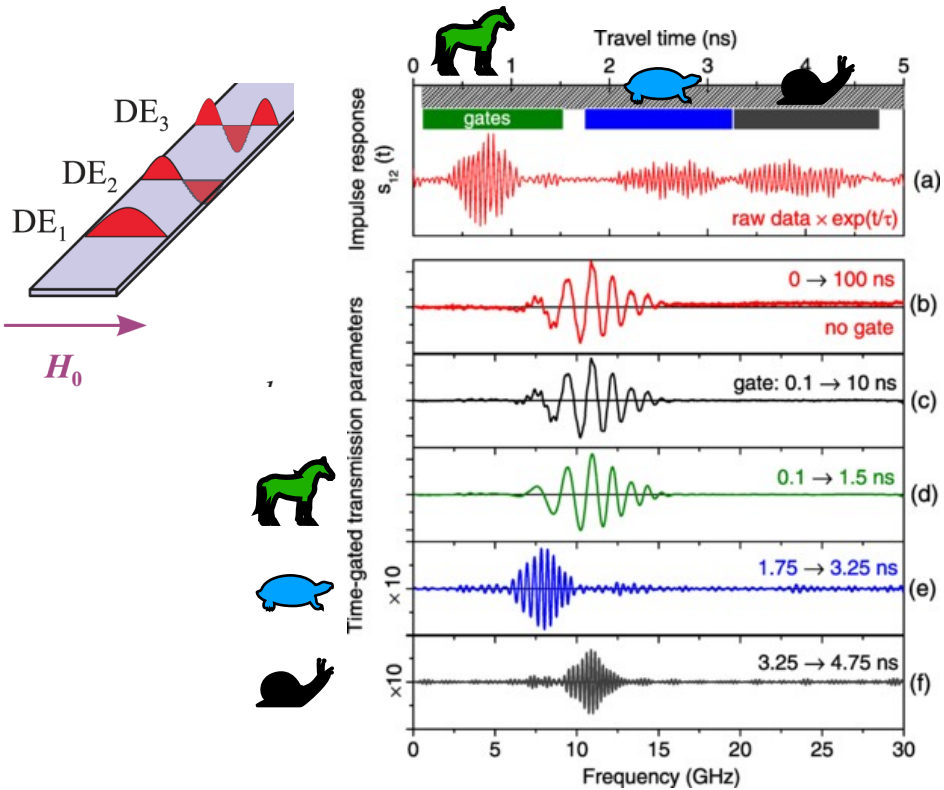

$$\tilde{S}_{ij}^{\text{MANY mode}}(\omega) \propto \sum_{\text{all SW branches}} \tilde{S}_{ij}^{\text{single mode}}(\omega)$$

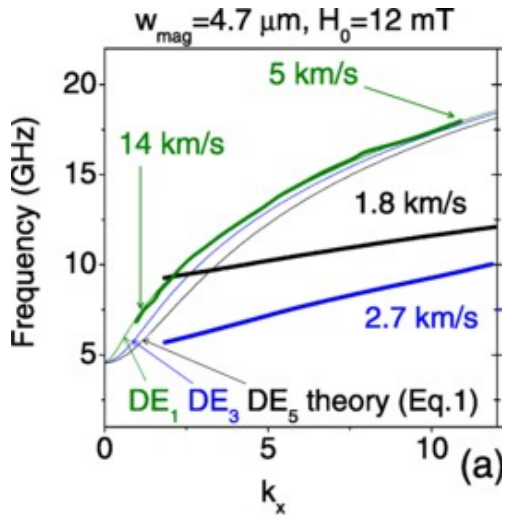

Now the spectrum of each wave packet matches with the single-mode model, so that unwrapping of {phase vs. freq} provides the dispersion relations

T. Devolder et al. *Phys. Rev. B* **103**, 214431 (2021)

Outline

- **Electrical techniques**
  - Broadband and cavity ferromagnetic resonance
  - Propagating spin-wave spectroscopy
  - Magneto-resistive detection of spin-waves
- **Optical techniques**
  - Time-resolved magneto-optical Kerr effect
  - Time-resolved X-ray imaging
  - Brillouin light scattering
- **Scanning probe techniques**
  - Magnetic resonance force microscopy
  - NV magnetometry

Spin torque driven ferromagnetic resonance in a nano-pillar

$$\frac{d\hat{m}}{dt} = -\gamma \hat{m} \times \mu_0(\vec{H}_{\text{eff}} + \vec{h}_{\text{Oe}}(\omega)) + \gamma \frac{1}{M_s t_{\text{FM}}} J_s(\omega)[\hat{m} \times (\hat{\sigma} \times \hat{m})] + \alpha \hat{m} \times \frac{d\hat{m}}{dt}$$

$I_{\text{rf}}(\omega)$

θ, β

$$V_{\text{dc}} = \langle R_{\text{rf}}(t) I_{\text{rf}}(t) \rangle$$
$$= \tfrac{1}{4}(R_{\text{AP}} - R_{\text{P}}) I_{\text{rf}} \sin\beta \sin\theta$$

V_{dc} (V)

$\omega = \omega_0$

→ magneto-resistive detection of magnetization dynamics very sensitive at the nanoscale

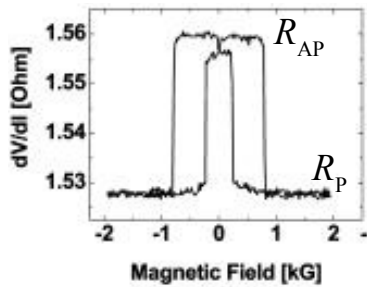

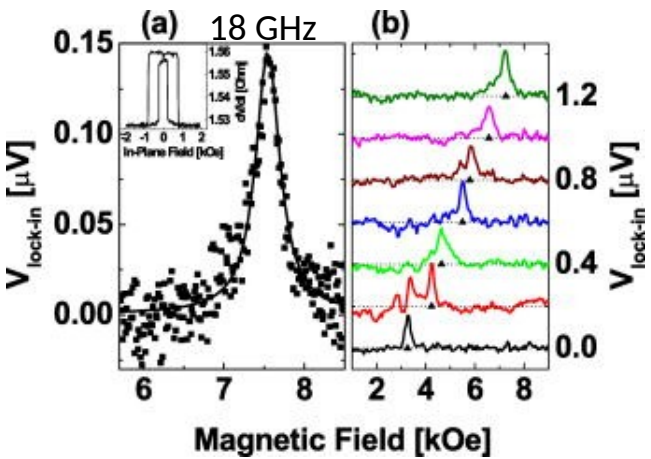

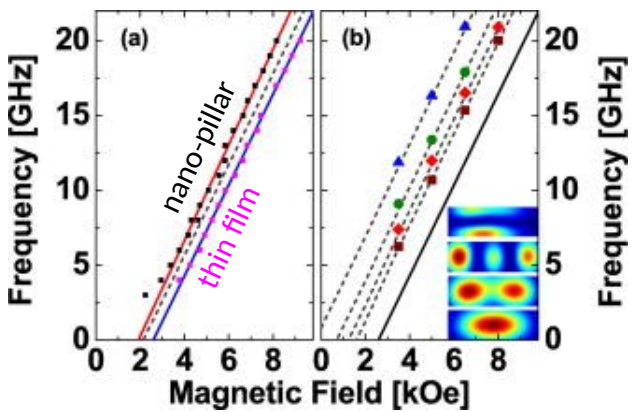

nano-pillar
50x150 nm²

thin film
~ mm

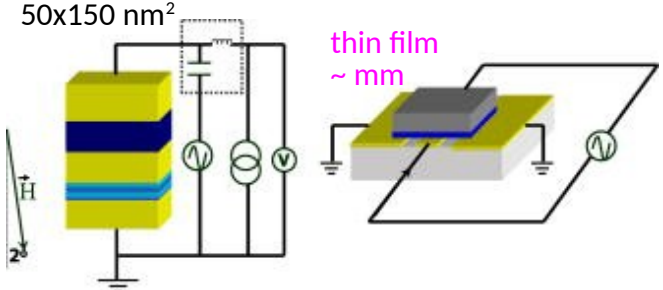

W. Chen et al. *J. Appl. Phys.* **103**, 07A502 (2008)

Electrical detection of FMR in insulating material

Adjacent normal metal layer (NM) to a ferromagnetic layer (FM)
→ additional channel of relaxation for spin-wave excitations

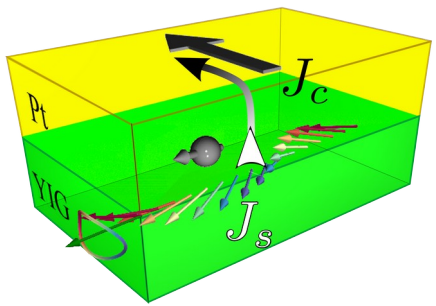

Spin current pumped out of FM.

$$\boldsymbol{J}_s = \left(\frac{\hbar}{2eM_s}\right)^2 G_{\uparrow\downarrow}\left[\boldsymbol{M}\times\frac{\partial \boldsymbol{M}}{\partial t}\right]$$

Interfacial increase of damping:

$$\alpha = \alpha_0 + \frac{\gamma\hbar}{4\pi M_s t_{\mathrm{YIG}}}\frac{G_{\uparrow\downarrow}}{G_0}$$

Interfacial effect: also works if FM = insulator!

Spin-to-charge conversion by inverse spin Hall effect if NM with strong spin orbit interaction.

$$\boldsymbol{J}_c = \frac{2e}{\hbar}\Theta_{\mathrm{SH}}[\boldsymbol{y}\times\boldsymbol{J}_s]$$

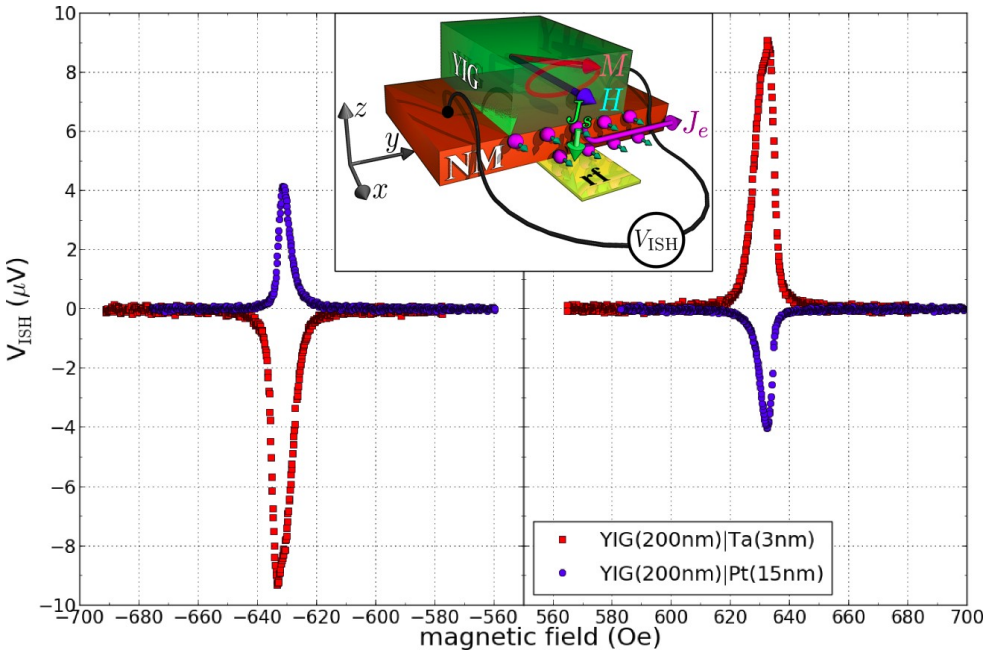

C. Hahn et al. *Phys. Rev. B* **87**, 174417 (2013)

ISHE-detected FMR spectroscopy in YIG/Pt microdiscs

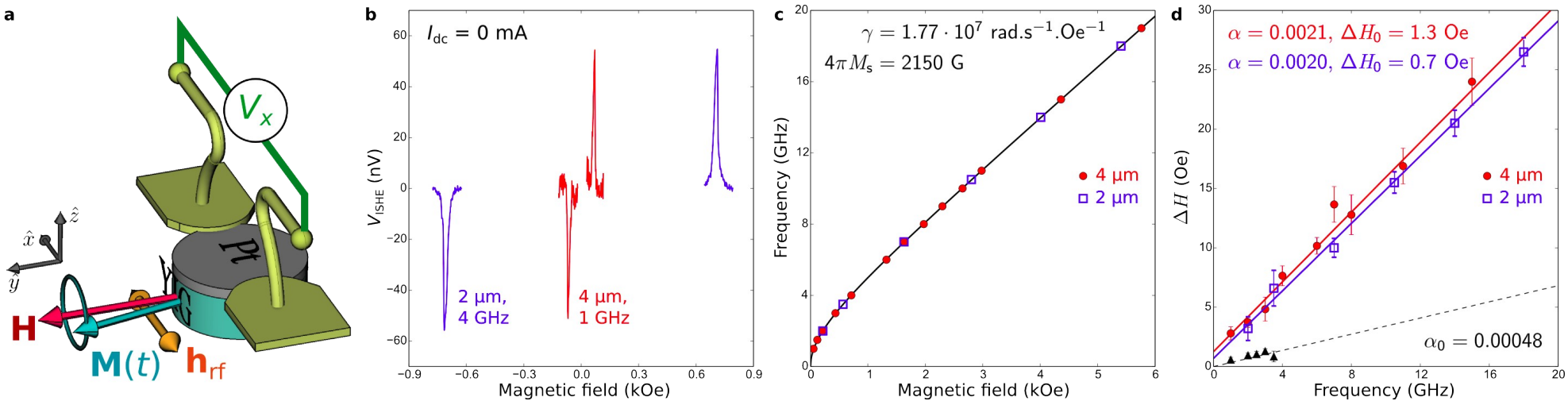

M. Collet et al. *Nat. Commun.* **7**, 10377 (2016)

Outline

- **Electrical techniques**
  - Broadband and cavity ferromagnetic resonance
  - Propagating spin-wave spectroscopy
  - Magneto-resistive detection of spin-waves
- **Optical techniques**
  - Time-resolved magneto-optical Kerr effect
  - Time-resolved X-ray imaging
  - Brillouin light scattering
- **Scanning probe techniques**
  - Magnetic resonance force microscopy
  - NV magnetometry

Magneto-optical Kerr effect (MOKE)

Change in light polarization characteristics after reflection on a magnetic material

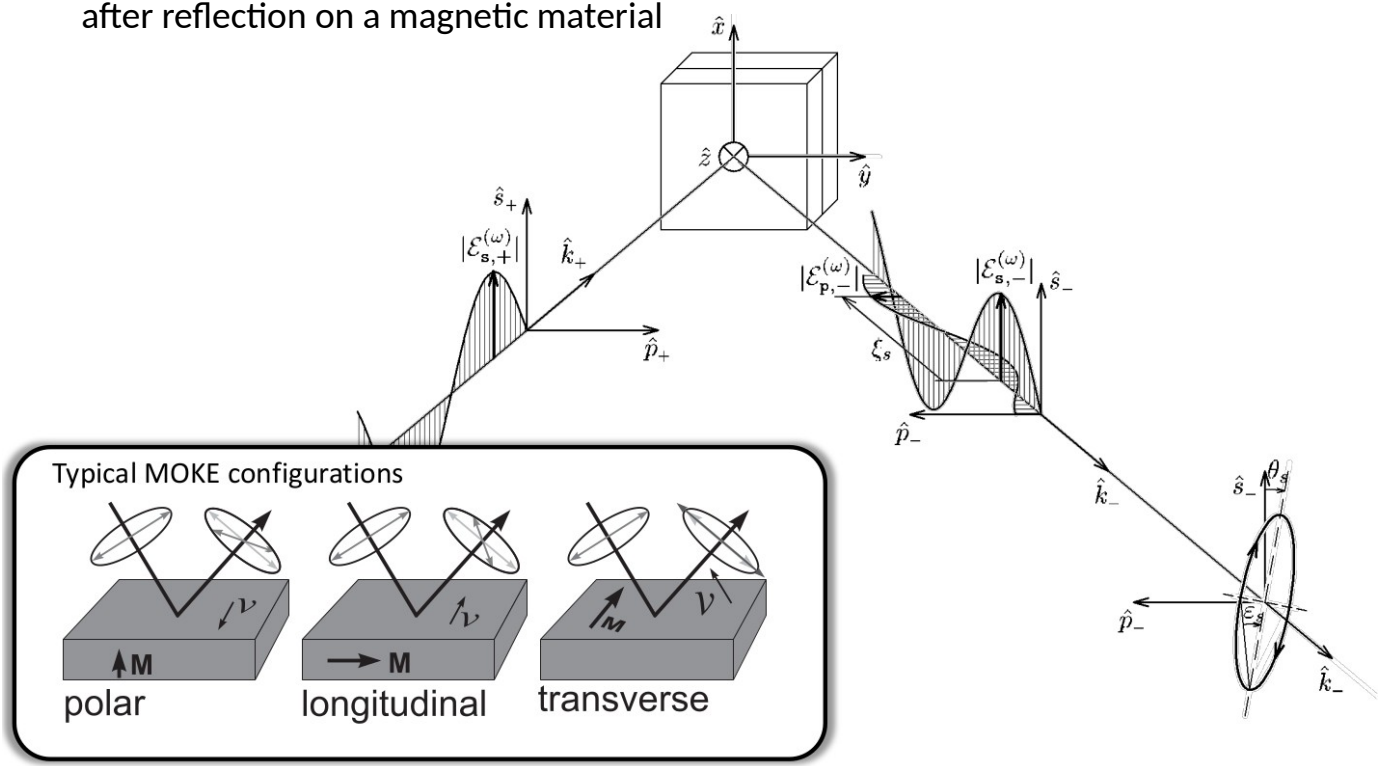

Imaging of magnetic domains

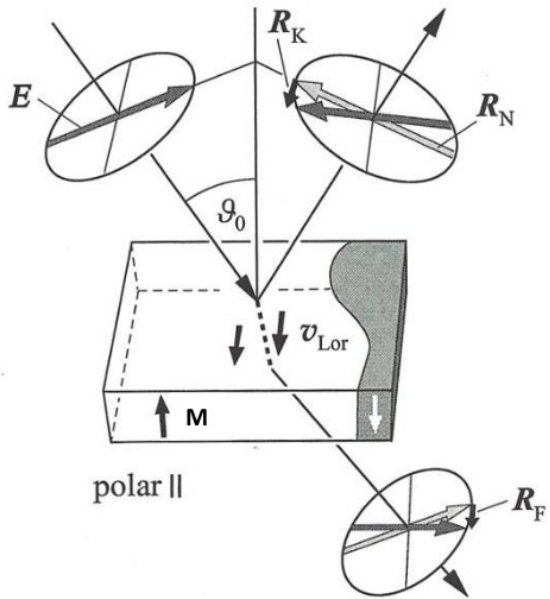

J. Harmle, *PhD* thesis (2003)
G. Woltersdorf, *PhD* thesis (2004)

A. Hubert & R. Schäfer, *Magnetic Domains*, Springer-Verlag (1998)

MOKE: macroscopic (classical) understanding

Can be understood with the Lorentz concept:

Lorentz force for a particle of charge e and velocity v:

$$\vec{F}_L = e \cdot \vec{E} + e \cdot \vec{v} \times q\vec{M}$$

in a magnetic material with a magnetization M (q : Voigt coefficient)

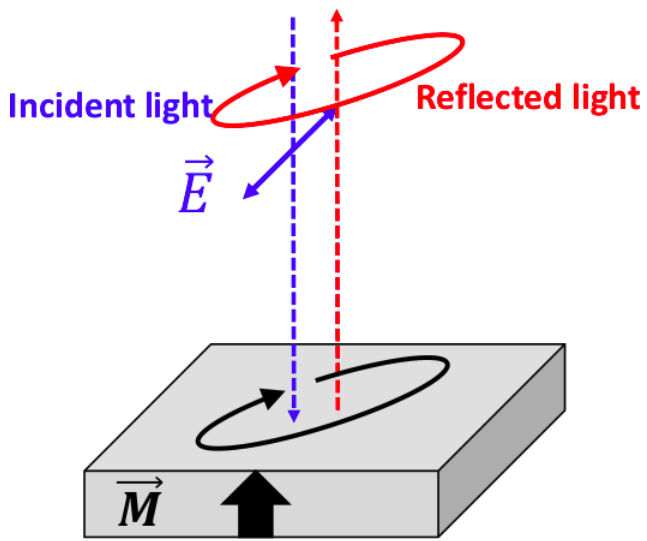

From Maxwell's equations in media:

$$\vec{D} = \varepsilon \cdot \vec{E}$$

$$\varepsilon = \varepsilon_0 \cdot \begin{pmatrix} 1 & iq \cdot M_z & -iq \cdot M_y \\ -iq \cdot M_z & 1 & iq \cdot M_x \\ iq \cdot M_y & -iq \cdot M_x & 1 \end{pmatrix}$$

ε : electric permittivity

MOKE: macroscopic (classical) understanding

Can be understood with the Lorentz concept:

Lorentz force for a particle of charge e and velocity v:

$$\vec{F}_L = e \cdot \vec{E} + e \cdot \vec{v} \times q\vec{M}$$

in a magnetic material with a magnetization M (q : Voigt coefficient)

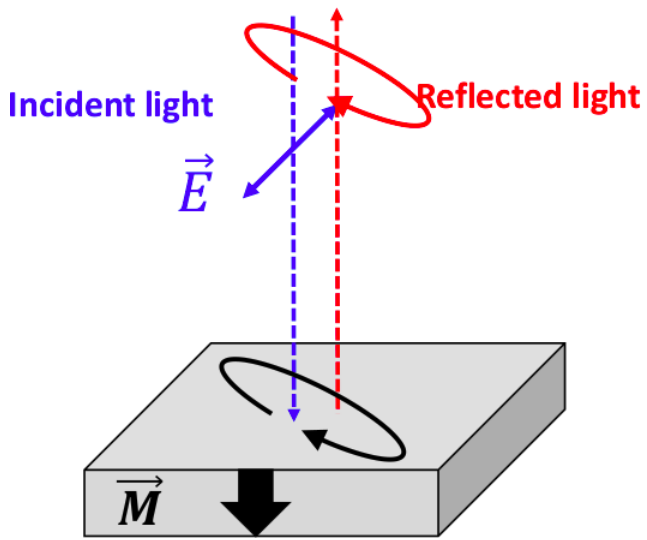

From Maxwell's equations in media:

$$\vec{D} = \varepsilon \cdot \vec{E}$$

$$\varepsilon = \varepsilon_0 \cdot \begin{pmatrix} 1 & iq \cdot M_z & -iq \cdot M_y \\ -iq \cdot M_z & 1 & iq \cdot M_x \\ iq \cdot M_y & -iq \cdot M_x & 1 \end{pmatrix}$$

ε : electric permittivity

Time-resolved scanning Kerr microscopy + ferromagnetic resonance

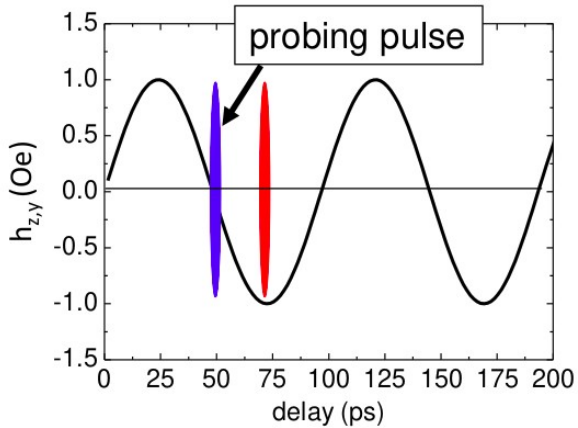

$$\chi_{zz,y} = \frac{m_z}{h_{z,y}}$$

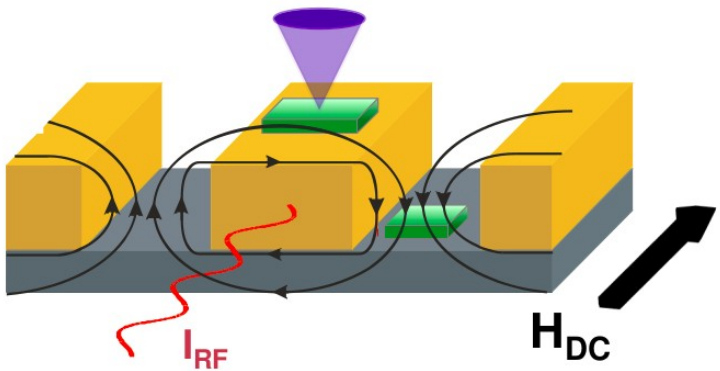

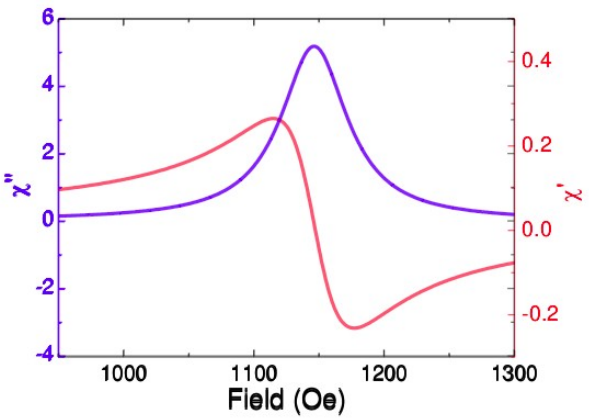

Time-resolved MOKE set-up

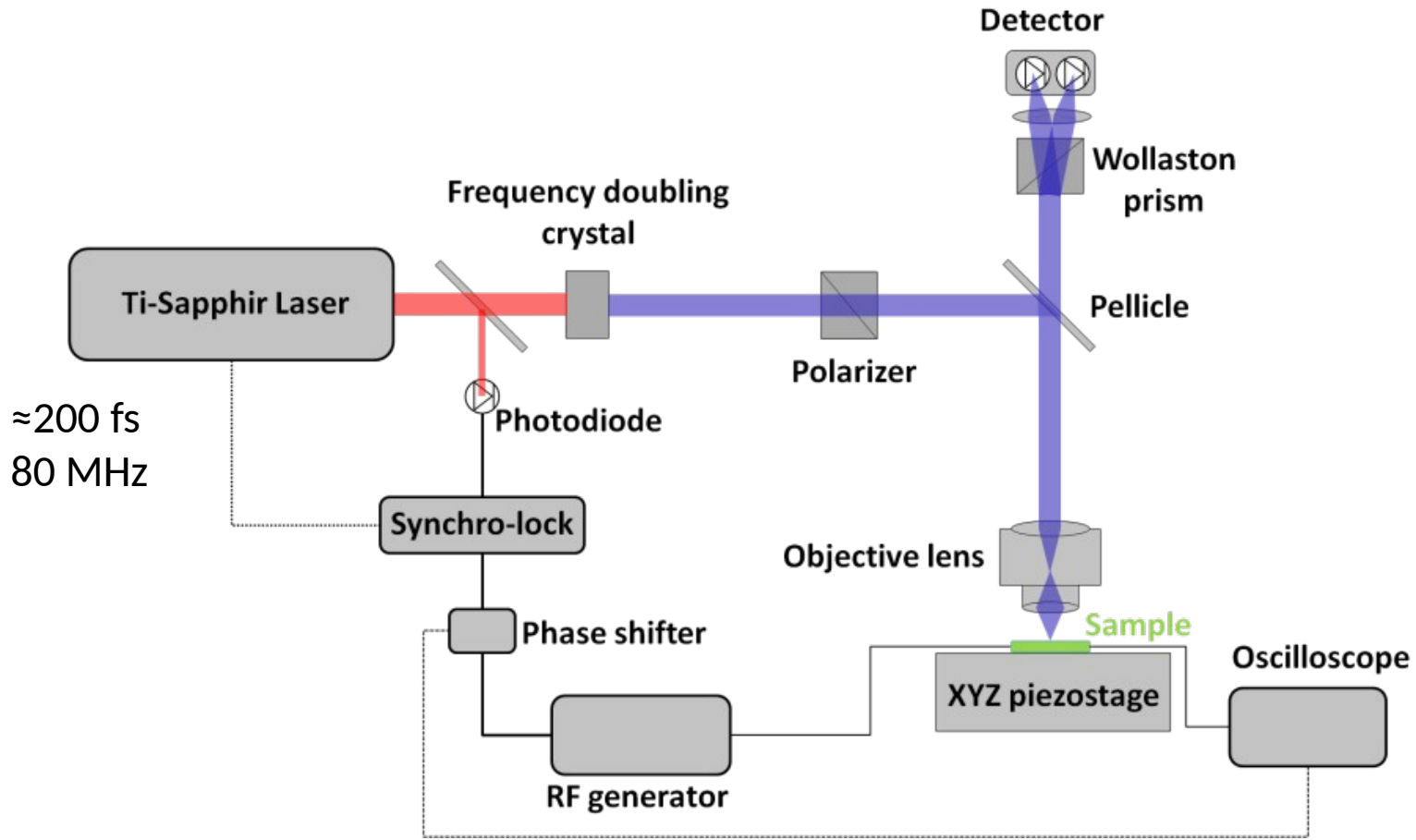

Time-resolved scanning Kerr microscopy + ferromagnetic resonance

Example:

- ***FMR spectrum :***

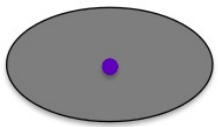

Py ellipse (15 µm x 7.5 µm)

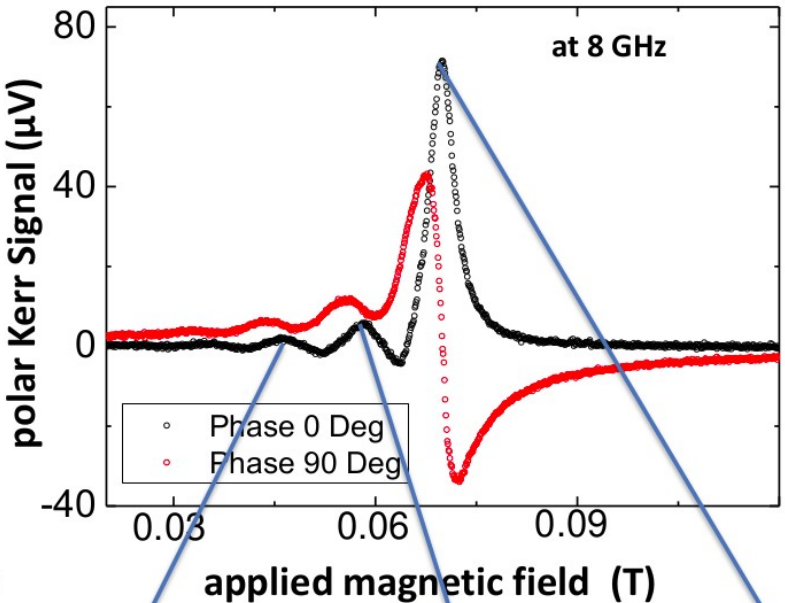

- ***Modes imaging :***

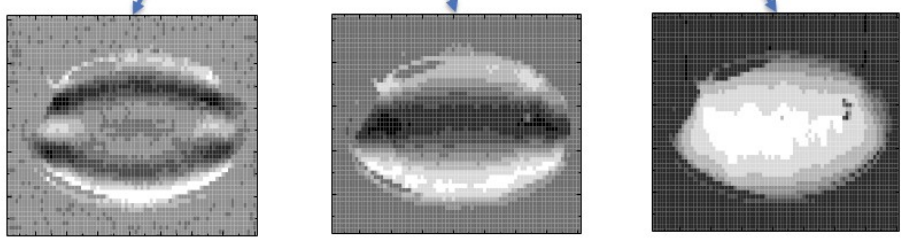

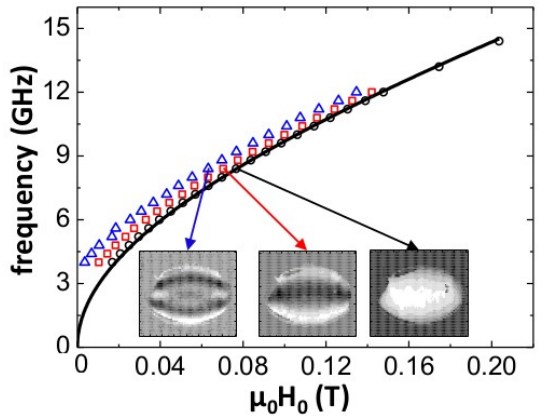

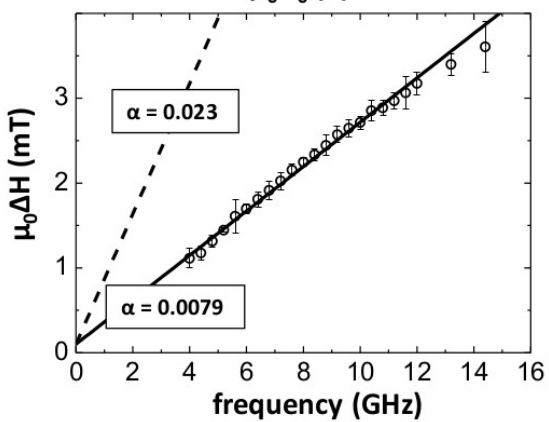

T. Weindler et al. *Phys. Rev. Lett.* **113**, 237204 (2014)

Spatio-temporal imaging of spin-wave eigenmodes

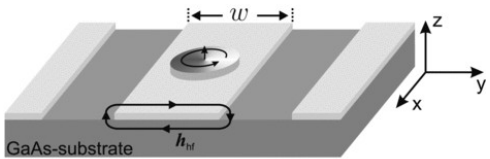

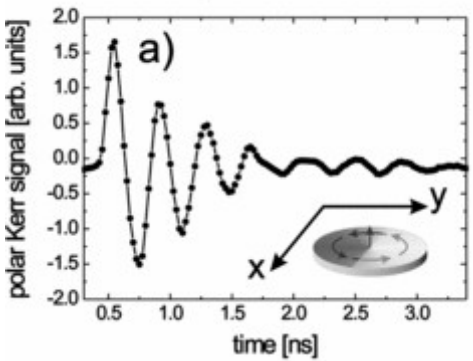

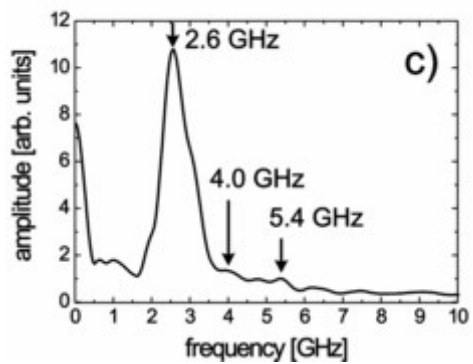

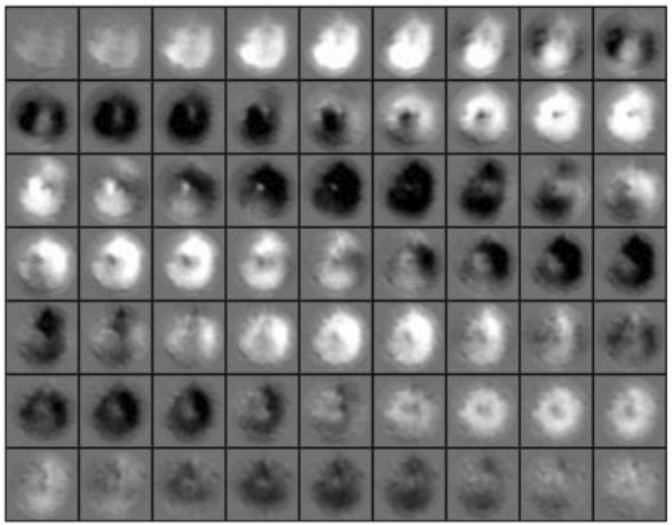

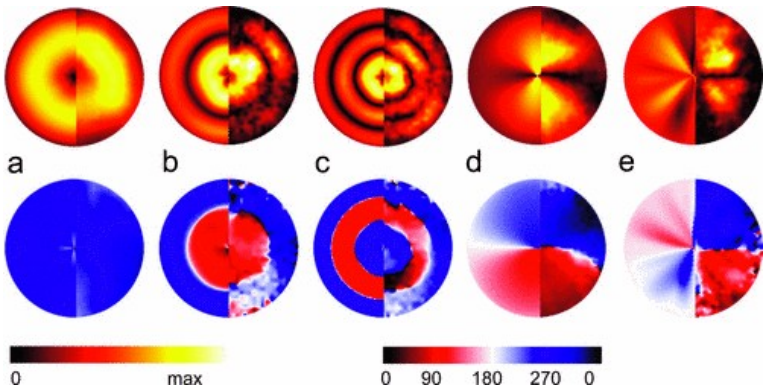

I. Neudecker et al. *Phys. Rev. B* **73**, 134426 (2006)

M. Buess et al. *Phys. Rev. Lett.* **93**, 077207 (2004)

M. Buess et al. *Phys. Rev. B* **71**, 104415 (2005)

Time-resolved scanning Kerr microscopy of propagating spin-waves

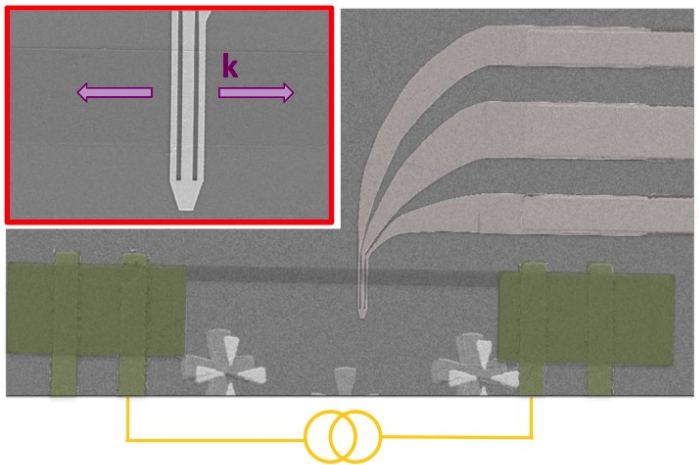

RF excitation
- 4 GHz ... 15 GHz
- phase modulation

Applied Field
(Rq : Damon-Eshbach geometry)

DC applied current
- few mA
- 2 polarities

Py stripes : width (0.8-2.5µm) , thickness (10-20 nm)
Au antenna : signal line 600*60 nm²
50 nm Al_2O_3 between Py and Au

Spinwave resonance spectrum

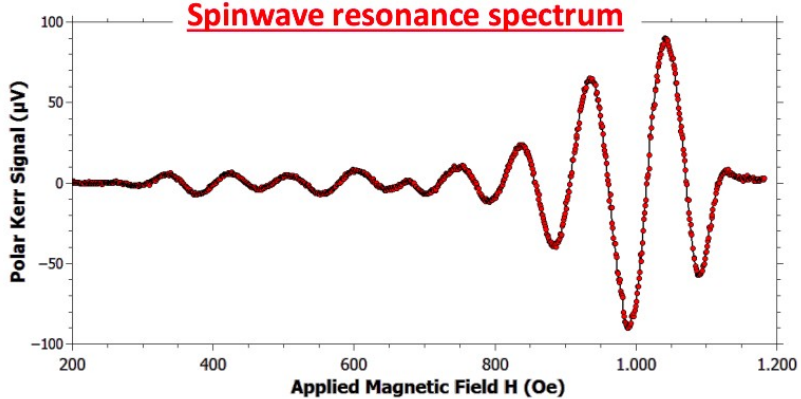

Spinwave magnetic imaging

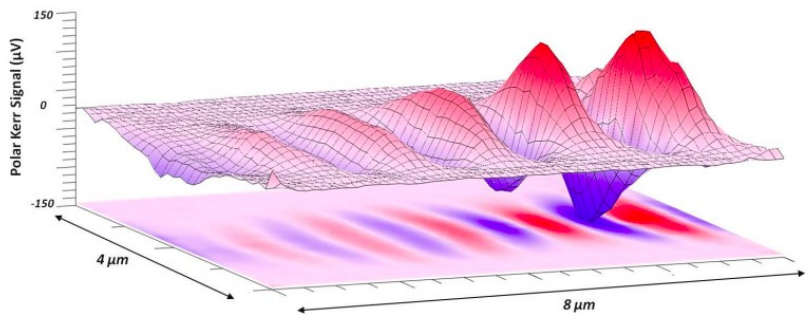

J.-Y. Chauleau et al. *Phys. Rev. B* **89**, 020403(R) (2014)

Time-resolved scanning Kerr microscopy of propagating spin-waves

800 nm x 12 nm stripe

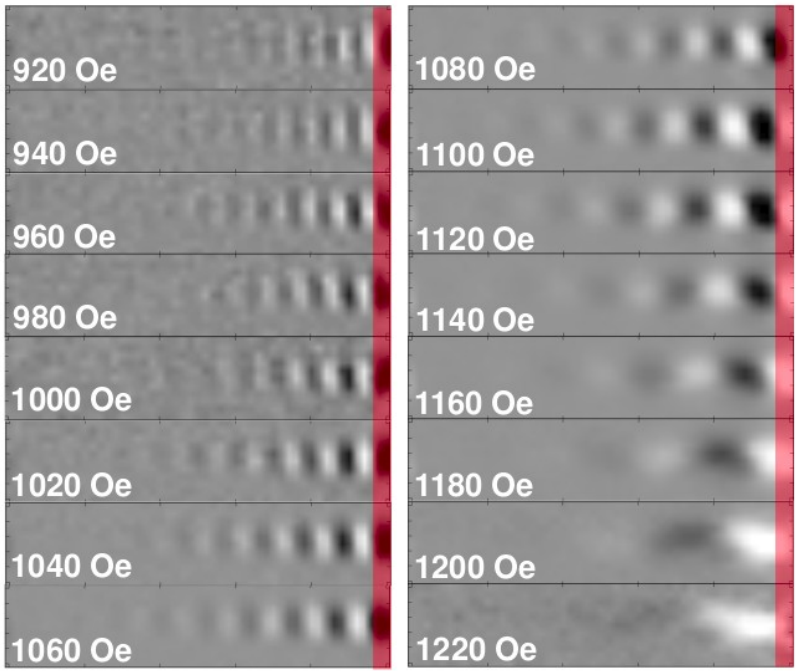

2500 nm x 20 nm stripe

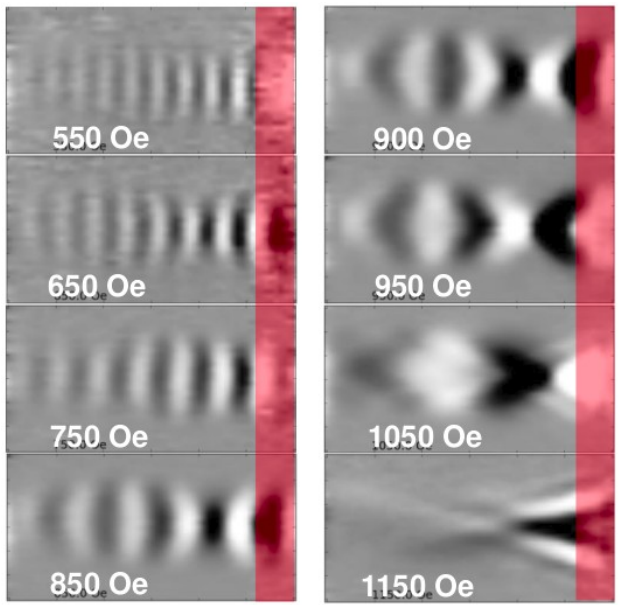

J.-Y. Chauleau et al. *Phys. Rev. B* **89**, 020403(R) (2014)

Outline

- **Electrical techniques**
  - Broadband and cavity ferromagnetic resonance
  - Propagating spin-wave spectroscopy
  - Magneto-resistive detection of spin-waves
- **Optical techniques**
  - Time-resolved magneto-optical Kerr effect
  - Time-resolved X-ray imaging
  - Brillouin light scattering
- **Scanning probe techniques**
  - Magnetic resonance force microscopy
  - NV magnetometry

X-ray magnetic circular dichroism (XMCD)

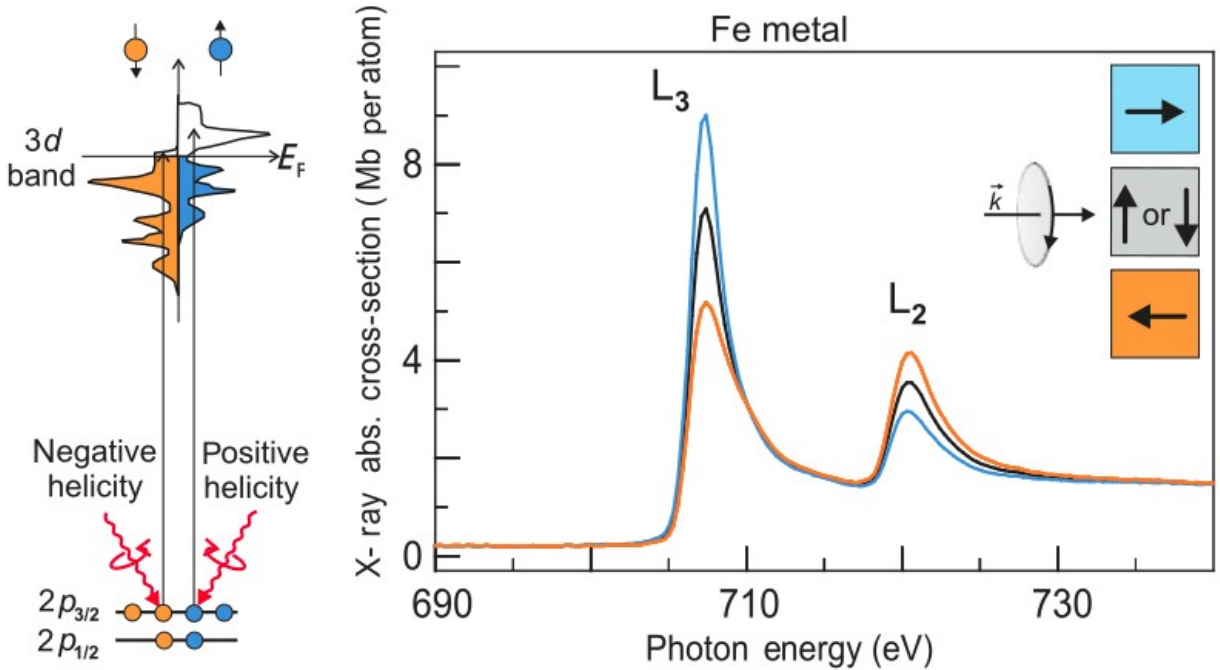

Element specific!

J. Stöhr & H. C. Siegmann, *Magnetism – From Fundamentals to Nanoscale Dynamics*, Springer-Verlag (2006)

Time-resolved scanning transmission X-ray microscopy

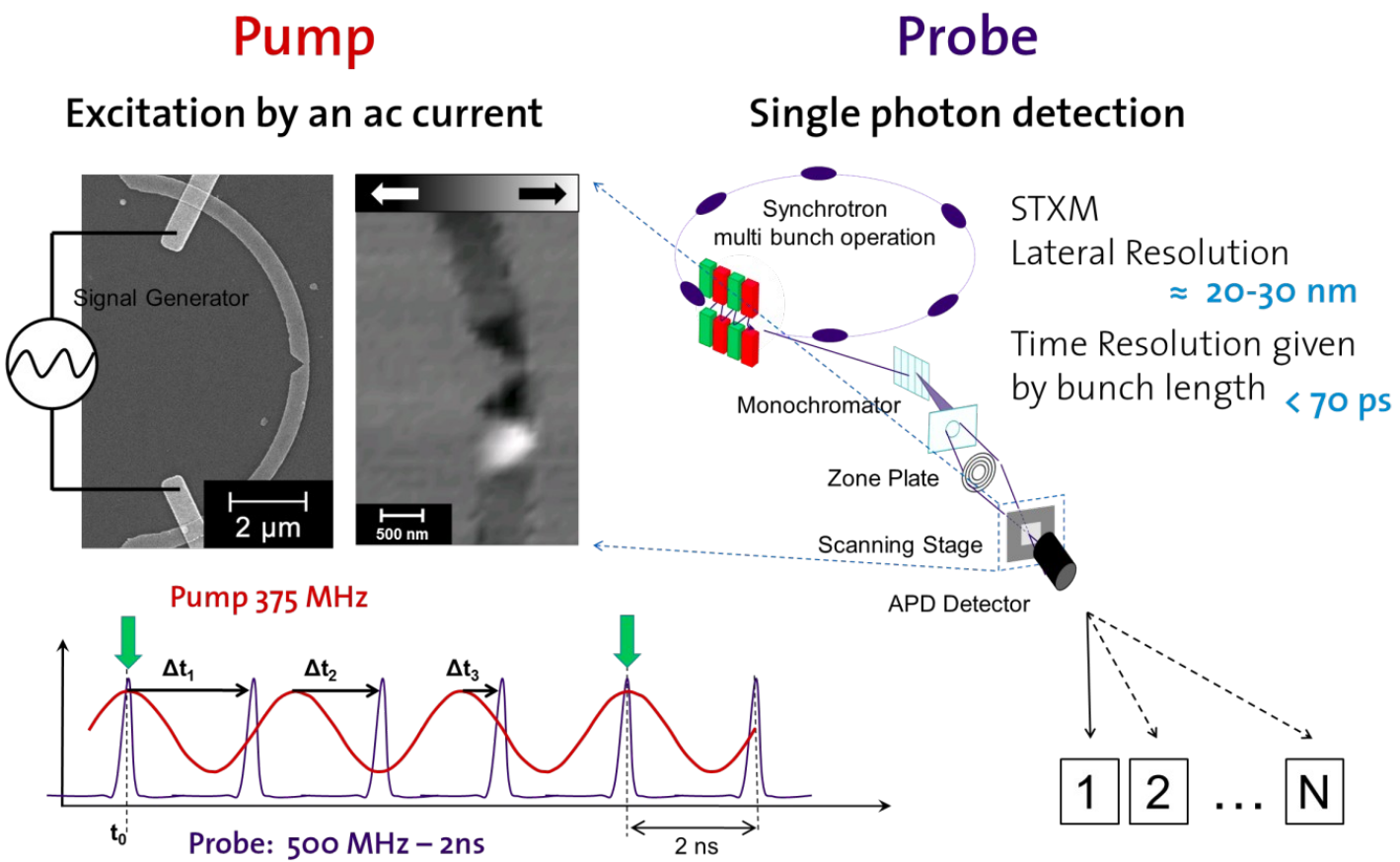

https://www.klaeui-lab.physik.uni-mainz.de/

Time-resolved X-ray imaging of nanoscale spin-wave dynamics

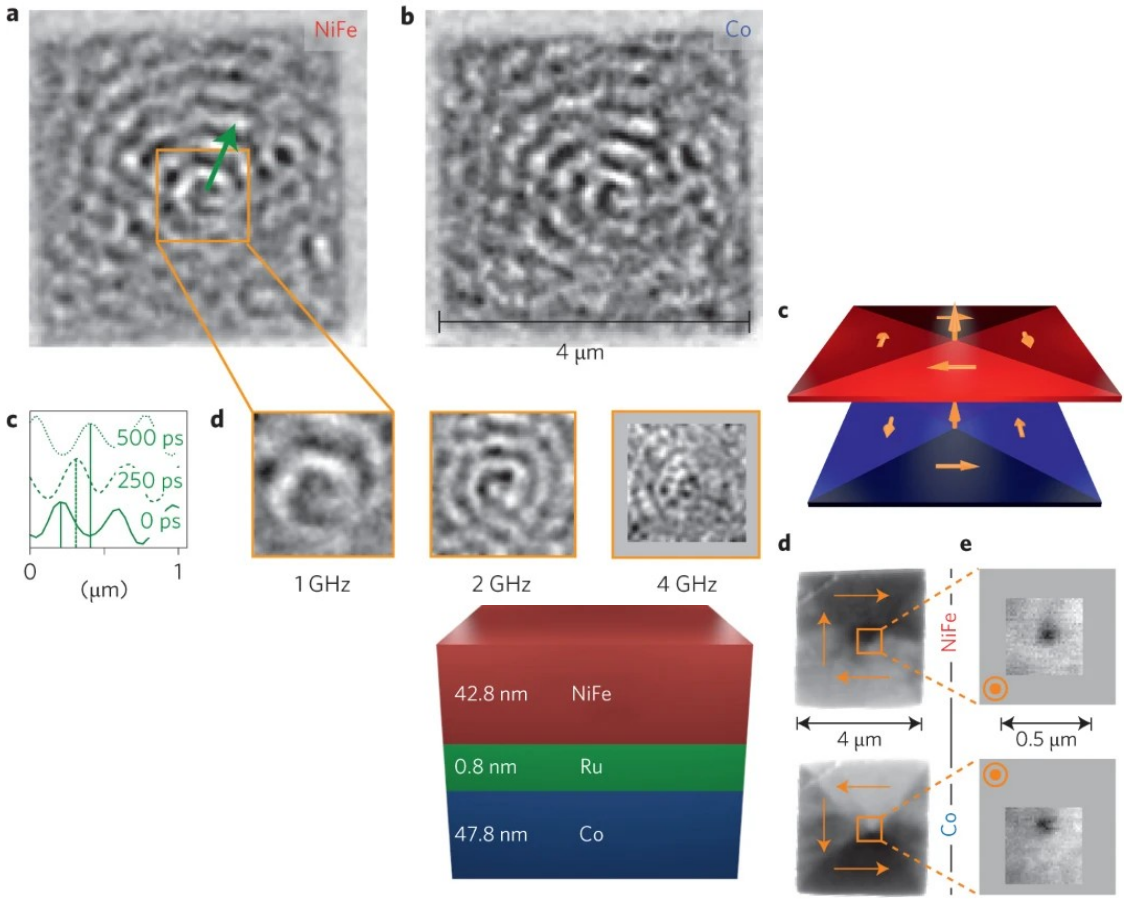

CoFeB disk t = 100 nm, R = 1 µm

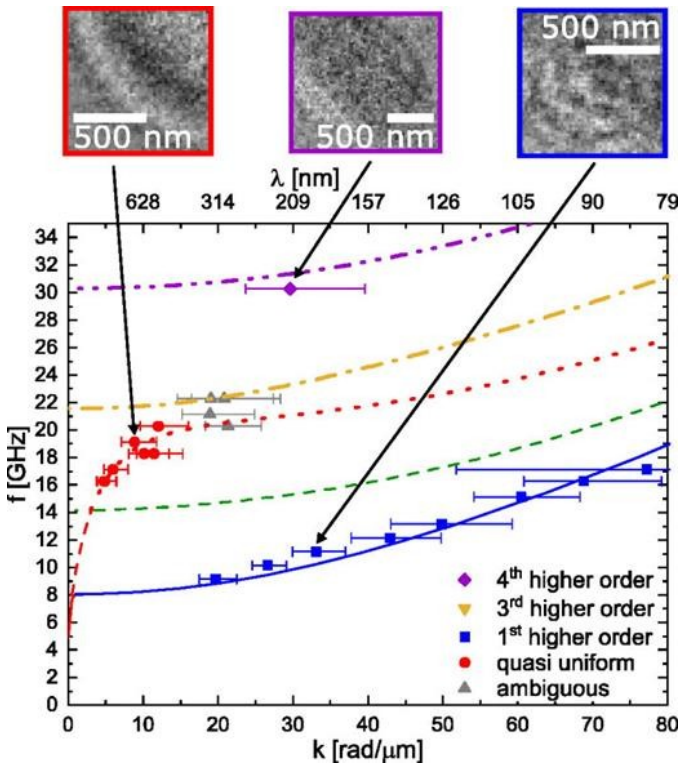

S. Wintz et al. *Nature Nanotech* **11**, 948 (2016)

S. Mayr et al. *Appl. Phys. Rev.* **11**, 041411 (2024)

Outline

- **Electrical techniques**
  - Broadband and cavity ferromagnetic resonance
  - Propagating spin-wave spectroscopy
  - Magneto-resistive detection of spin-waves
- **Optical techniques**
  - Time-resolved magneto-optical Kerr effect
  - Time-resolved X-ray imaging
  - Brillouin light scattering
- **Scanning probe techniques**
  - Magnetic resonance force microscopy
  - NV magnetometry

Brillouin light scattering (BLS)

PHYSIQUE MATHÉMATIQUE. — *Diffusion de la lumière par un corps transparent homogène.* Note de M. **Léon Brillouin**, présentée par M. J. Violle.

I. Lorsqu'un rayon lumineux traverse un corps isotrope, une partie de la lumière est diffusée dans toutes les directions. Ce phénomène, est visible dans le bleu du ciel (1) et dans l'opalescence critique (2). Je veux ici compléter la théorie donnée par Einstein (3) pour la mettre en accord avec les travaux de Debije (4) sur les chaleurs spécifiques.

Un corps homogène, à température fixe, est en continuelle vibration. On peut décomposer ce mouvement suivant les vibrations propres du corps. Debije attribue à chaque vibration propre une énergie moyenne qui dépend de sa période suivant la loi de Planck. Parmi ces vibrations, les ondes longitudinales produisent des écarts de densité capables de diffuser la lumière.

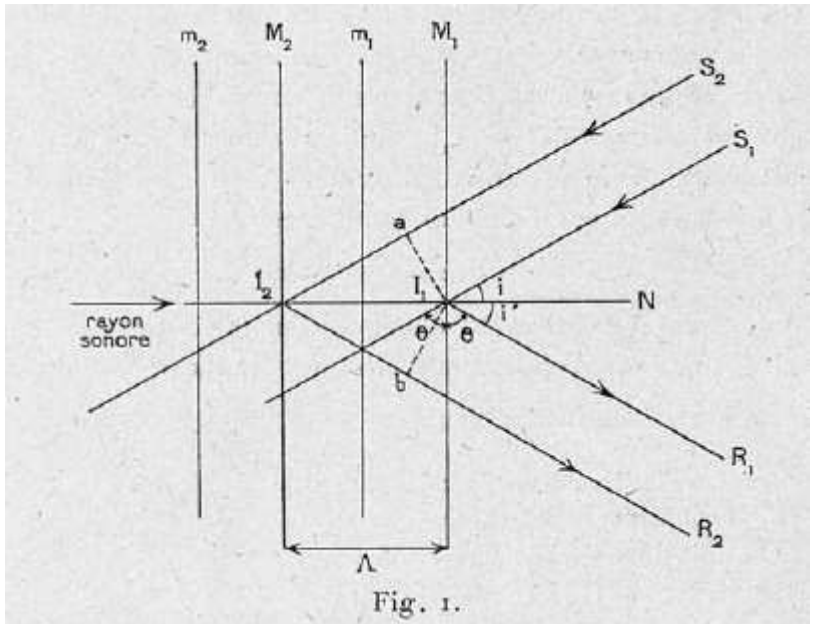

Fig. 1.

L. Brillouin, *Compt. Rend.* **158**, 1331 (1914)
Ann. Physique **9**, 88 (1922)

Photon – spin-wave interaction

Magnon creation
(Stokes process, energy loss)

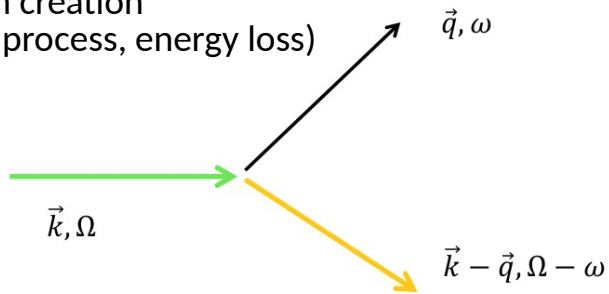

Magnon creation
(anti-Stokes process, energy gain)

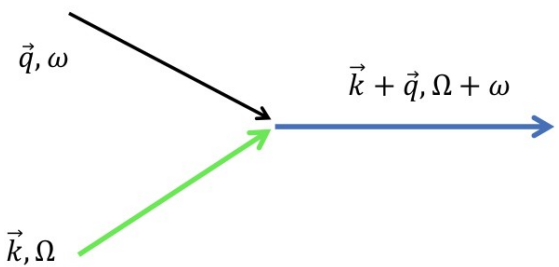

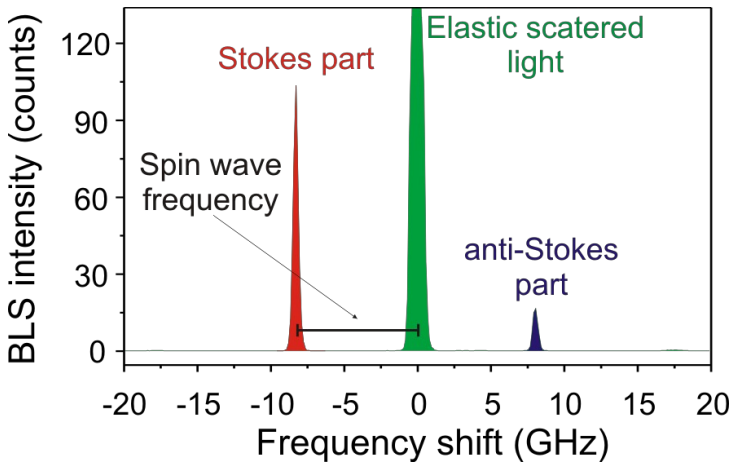

Intensity of the scattered light is proportional to magnon density

Interaction term: the magneto-optical effect

- First order magneto-optical effect $\vec{D} = \bar{\bar{\varepsilon}}\vec{E} + \vec{P}_M = \bar{\bar{\varepsilon}}\vec{E} + iQ\vec{E} \times \vec{M}$
- Static and dynamic magnetization $\vec{M} = \vec{M}_0(\vec{0}, 0) + \vec{m}(\vec{q}, \omega)$
- Magnetic scattering is cross-polarized $\vec{E}(\vec{k}, \Omega) \times \vec{m}(\vec{q}, \omega) \rightarrow \vec{P}_M(\vec{k} \pm \vec{q}, \Omega \pm \omega)$
- Scattering complex amplitude $\vec{E}_s^{\,*}.(\vec{E}_i \times \vec{m}) = \vec{m}.(\vec{E}_s^{\,*} \times \vec{E}_i)$

- Effect of phonons $\varepsilon = \bar{\bar{\varepsilon}}(\vec{0}, 0) + \delta\varepsilon(\vec{q}, \omega)\bar{\bar{I}}$ pressure wave

  Except for shear waves, phonon scattering is parallel-polarized

BLS on magnetic thin films

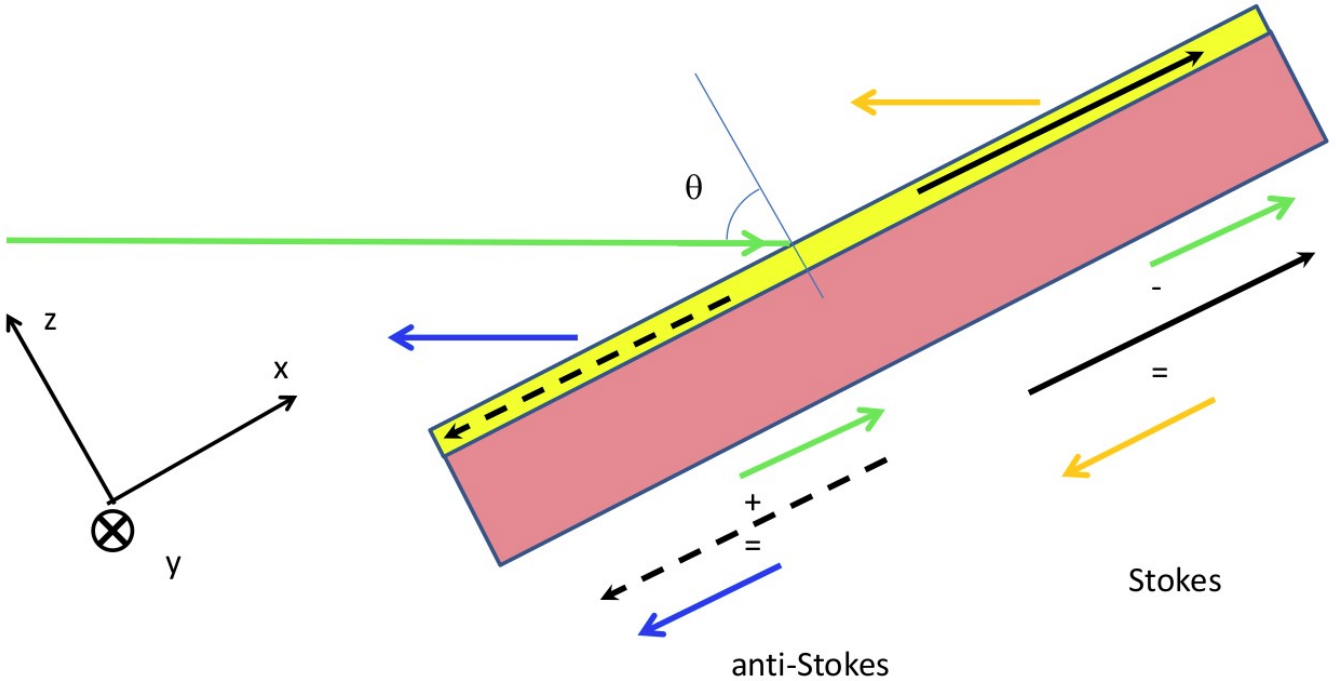

Thin film: spin-waves have only an in-plane wavevector
only the in-plane wavevector is conserved

Transferred wavevector $|\vec{q}| = 2 \times \frac{2\pi}{\lambda} \sin\theta$

Brillouin light scattering spectrometer

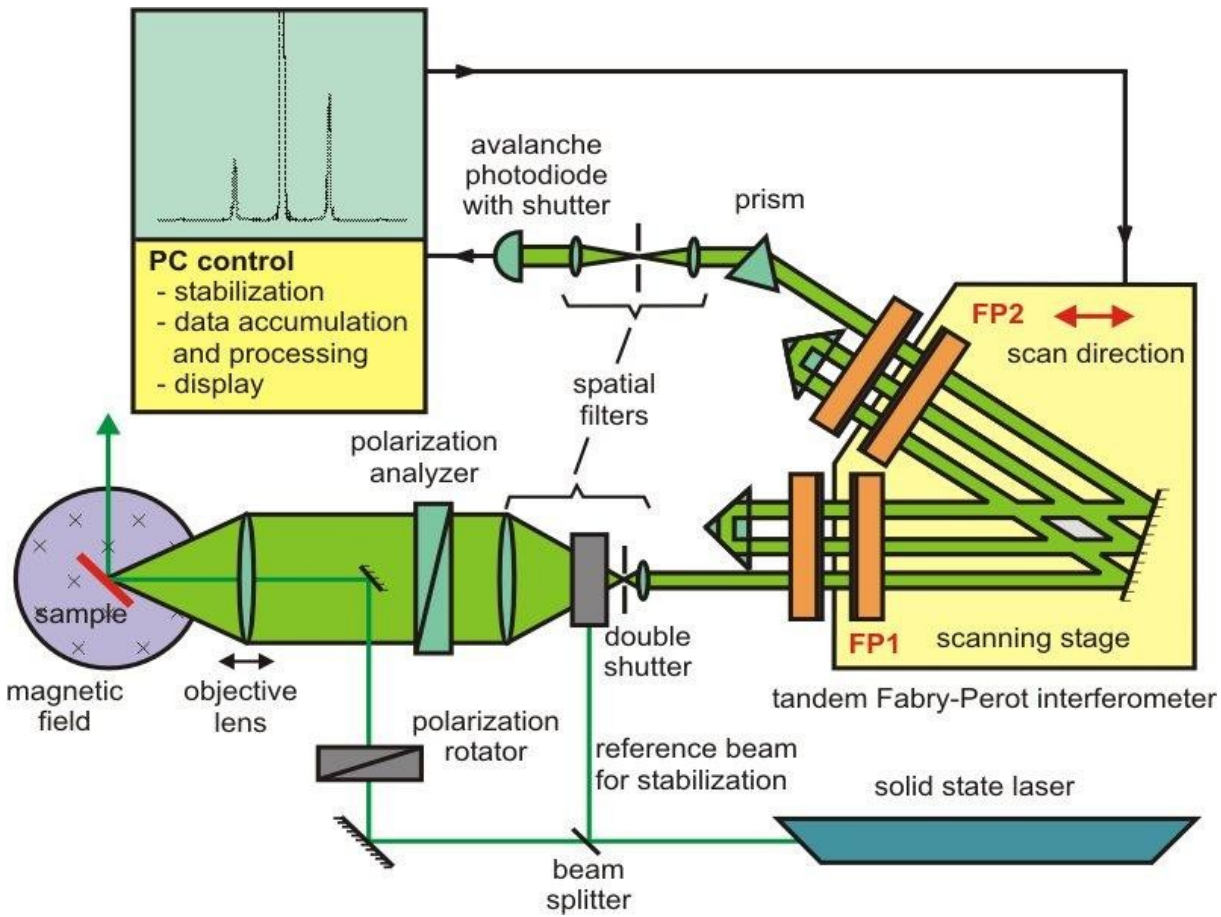

High-resolution interferometry with high contrast for measurements of acoustic phonons and spin waves.

Frequency (or wavelength) variations of the order of a ppm!

Can detect thermal spin-waves!

Illustration from B. Hillebrands' ESM2024 lecture

BLS measurements to extract magnetic parameters of ultra-thin films

Magnetic film: Pt/Co 1.1 nm/AlOx

$$f = \frac{\gamma}{2\pi}\sqrt{\left(B + \mu_0 M_s \frac{|q|t}{2} + \frac{2A}{M_s}q^2\right)\left(B - B_K - \mu_0 M_s \frac{|q|t}{2} + \frac{2A}{M_s}q^2\right)} \pm \frac{\gamma}{\pi}\frac{Dq}{M_s} \equiv f_0 \pm \frac{\Delta f}{2}$$

Angle series at 258 mT

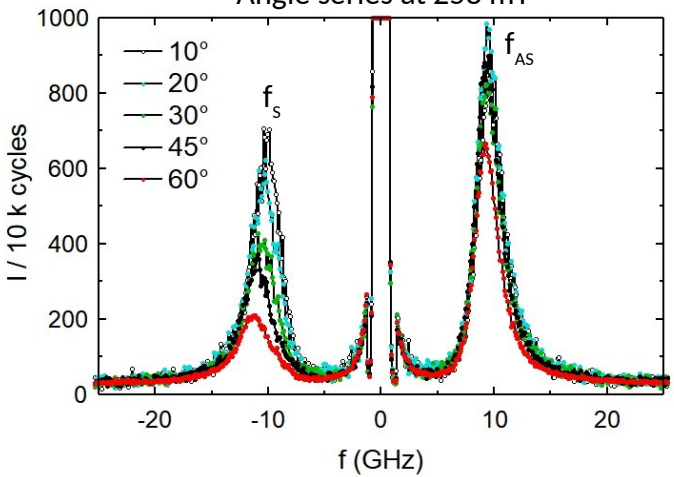

Central frequency

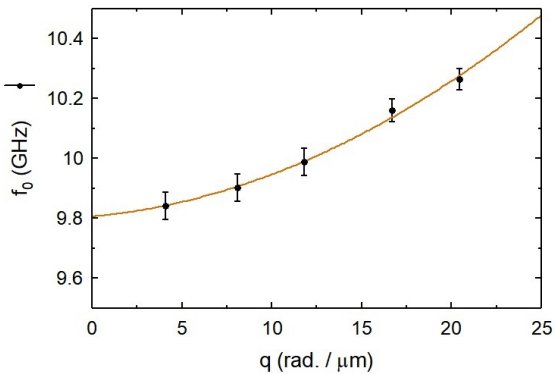

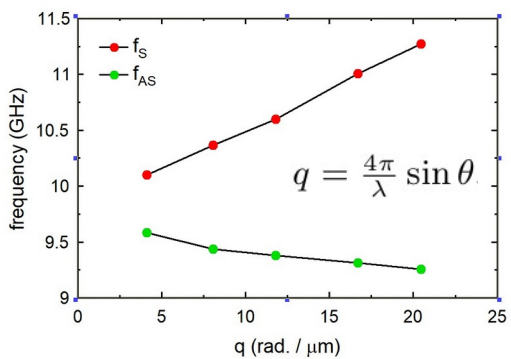

Frequency asymmetry

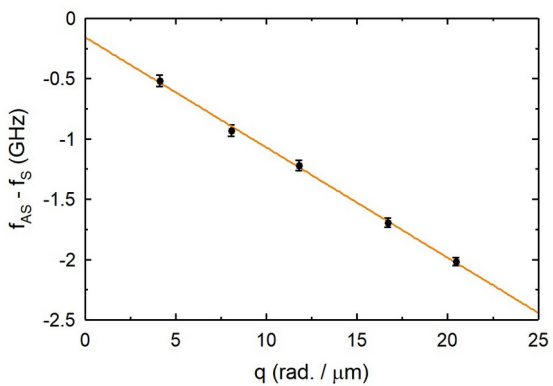

Parameters extracted from full BLS data set:

B_{Keff} = -0.173 +/- 0.01 T
$\Delta(B_{Keff})$ = 110 mT
(corresponds to 0.1 nm thickness fluctuation, and gives 1.5 GHz frequency fluctuation)

g = 2.11 +/- 0.02
α = 0.05

with M_s = 1 MA/m (B_s = 1.25 T)
A= 15 +/- 1 pJ/m
D= 0.77 +/- 0.02 mJ/m^2

C. Balen et al. *Small* **19**, 2302039 (2023)

Micro-focused Brillouin light scattering

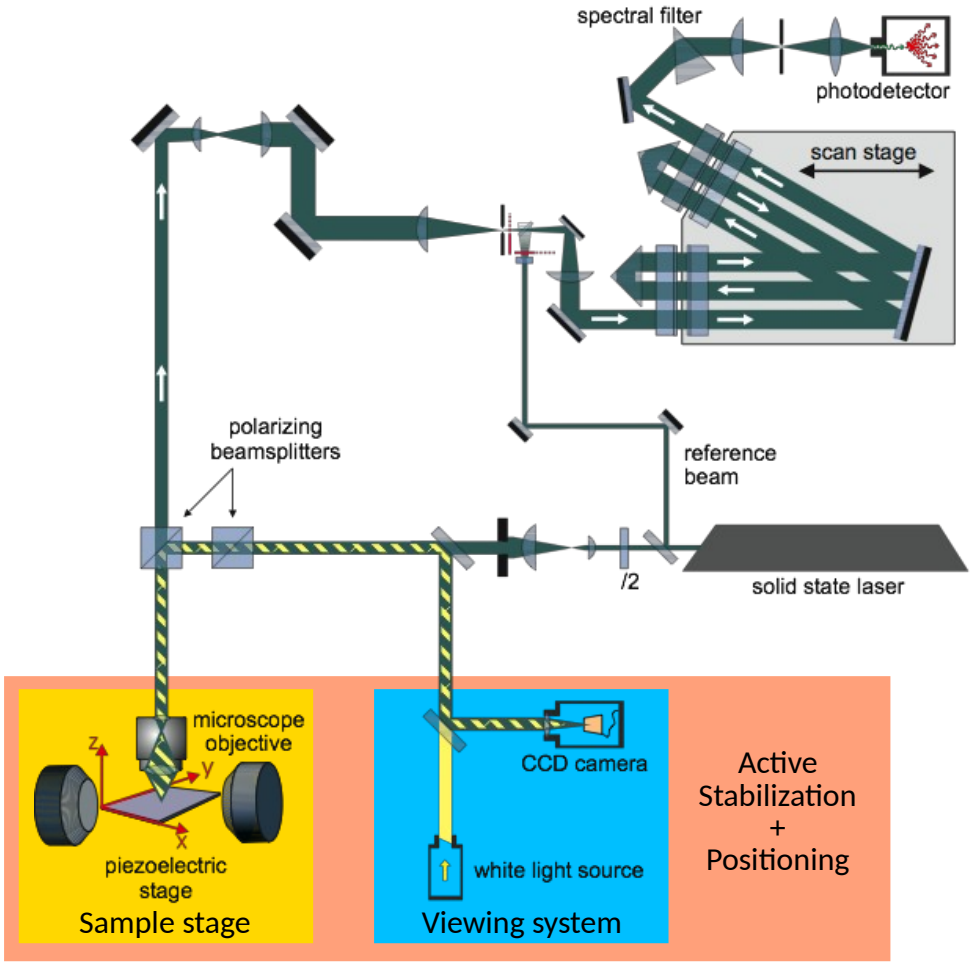

- optical resolution: 250 nm
- 2D piezo stage
- controlling sample while measuring, < 20 nm accuracy, long term stability
- frequency range: 1 GHz – 1 THz
- spectral resolution: 100 MHz

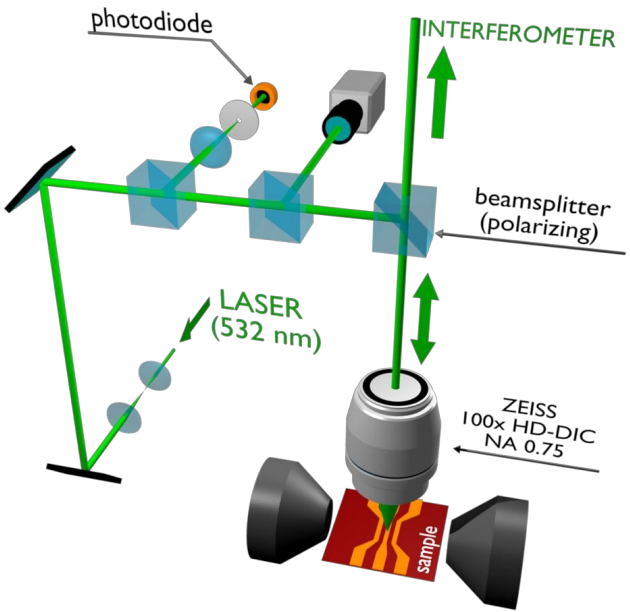

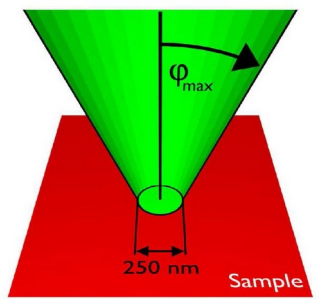

Illustration from B. Hillebrands' ESM2024 lecture

T. Sebastian et al. *Frontiers in Physics* **3**, 35 (2022)

Imaging the spatial profiles of spin-wave modes in microstructures

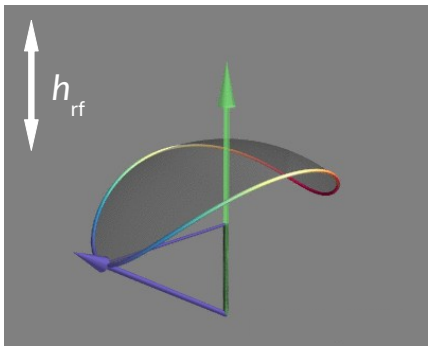

Parallel pumping → no selection rules

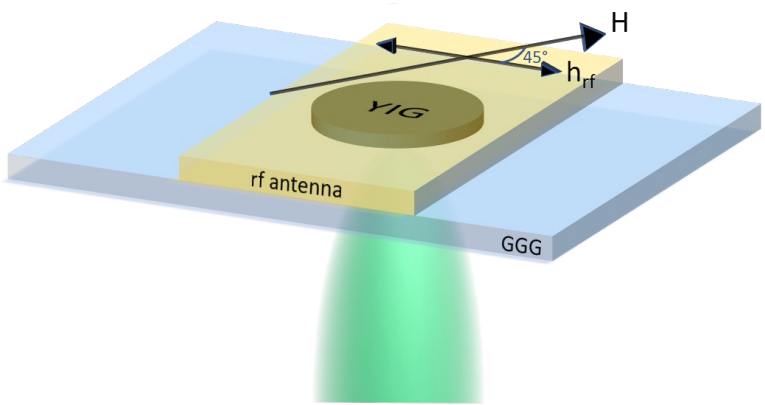

YIG disc: t = 50 nm, R = 1.5 μm

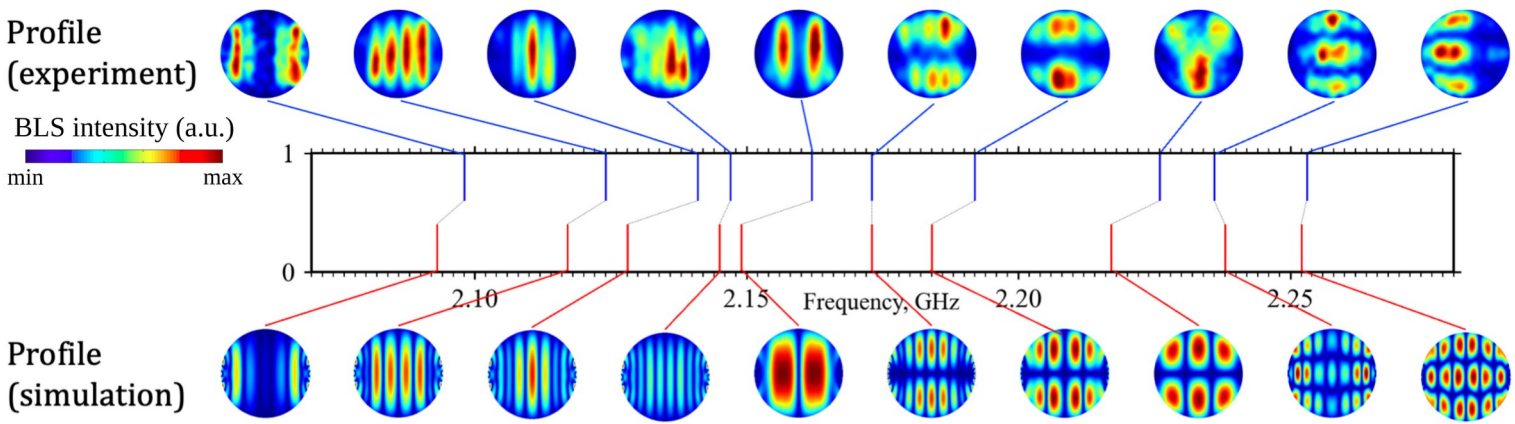

T. Srivastava et al. *Phys. Rev. Appl.* **19**, 064078 (2023)

Imaging propagating spin-waves in waveguides

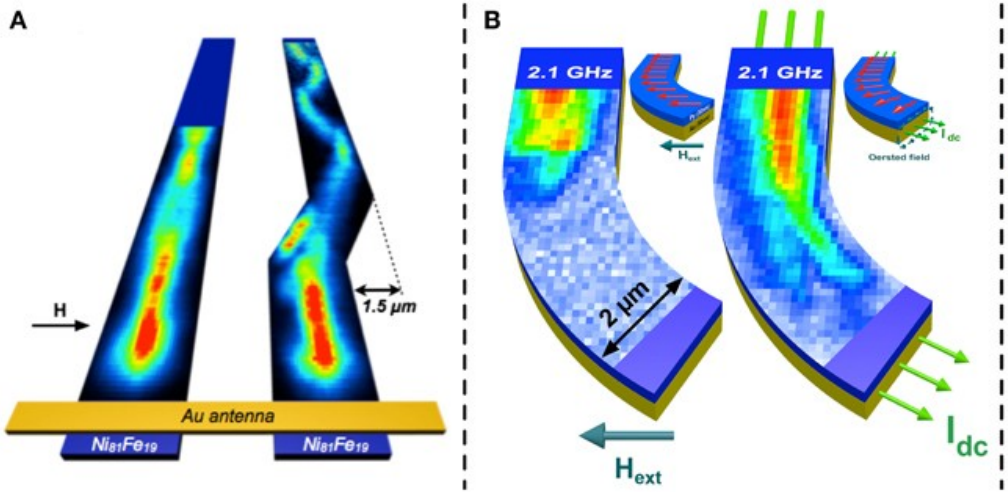

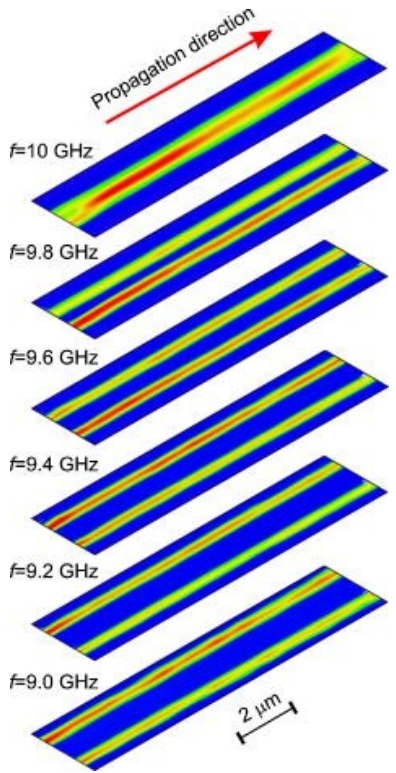

P. Clausen et al. *Appl Phys Lett.* **99**, 162505 (2011) K. Vogt et al. *Appl Phys Lett.* **101**, 042410 (2012); *Nat Commun.* **5**, 3727 (2014)

V. Demidov et al. *Appl. Phys. Lett.* **92**, 232503 (2008)

Time-resolved micro-focused BLS

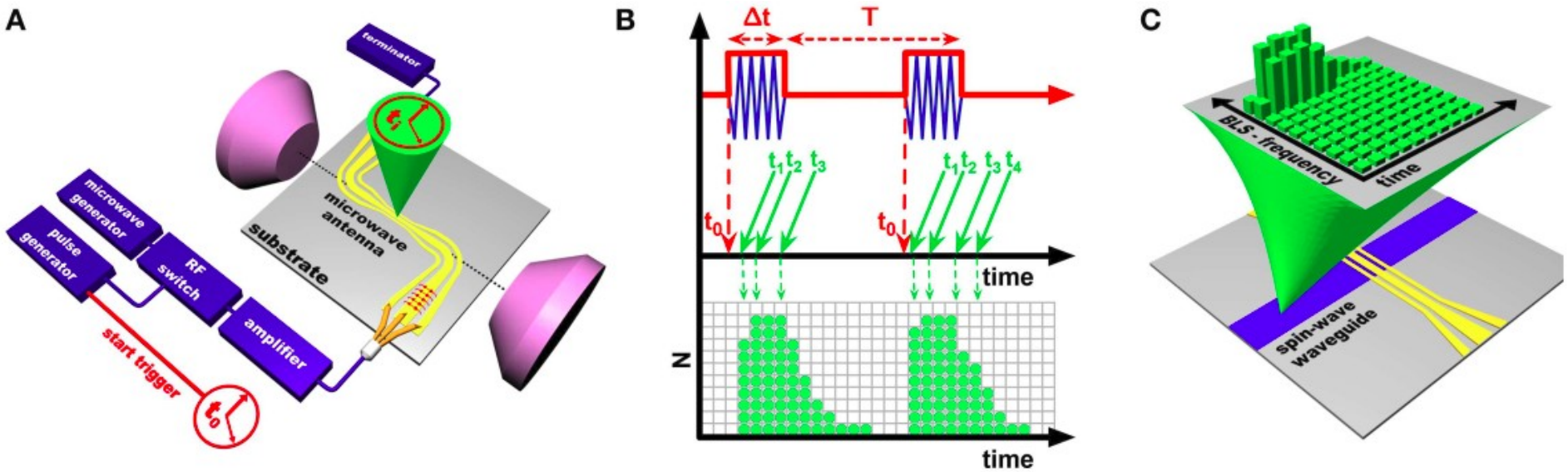

T. Sebastian et al. *Frontiers in Physics* **3**, 35 (2022)

Parametric excitation in YIG nanostructures

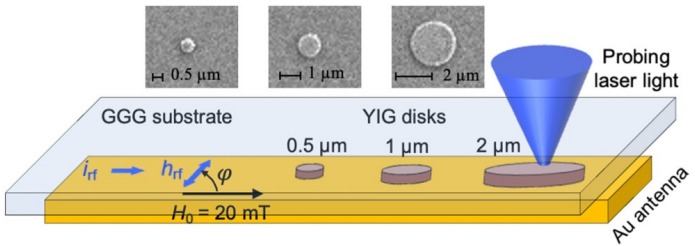

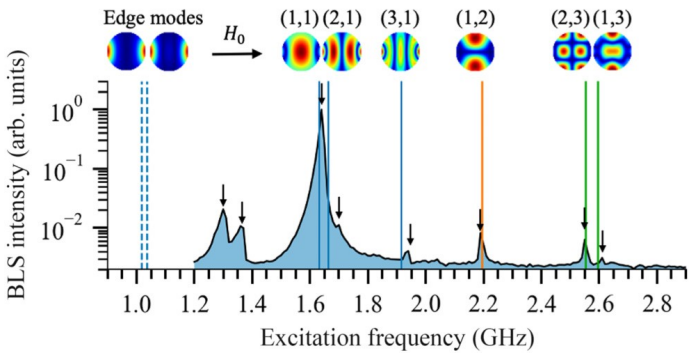

Direct linear excitation (0.5 µm disk)

Parallel parametric excitation (1 µm disk)

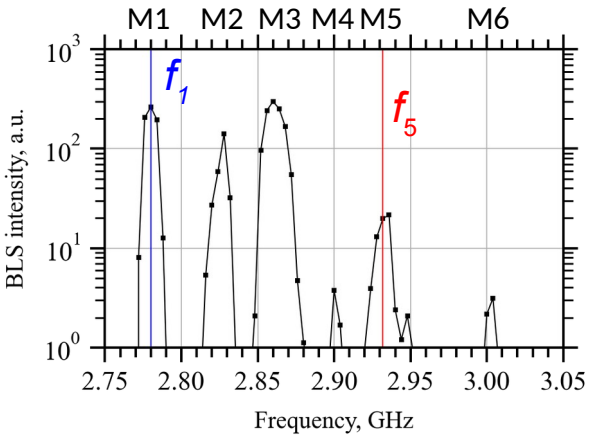

Mode amplitude vs. time

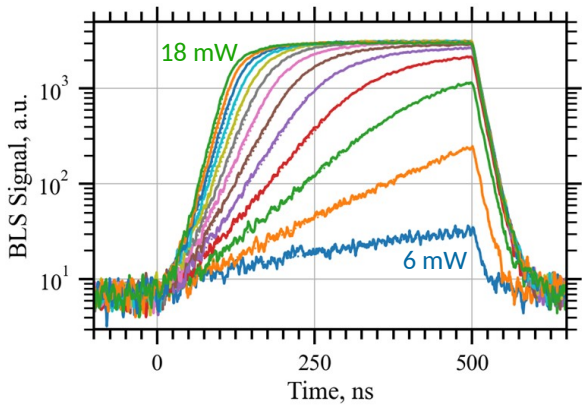

Double parametric excitation

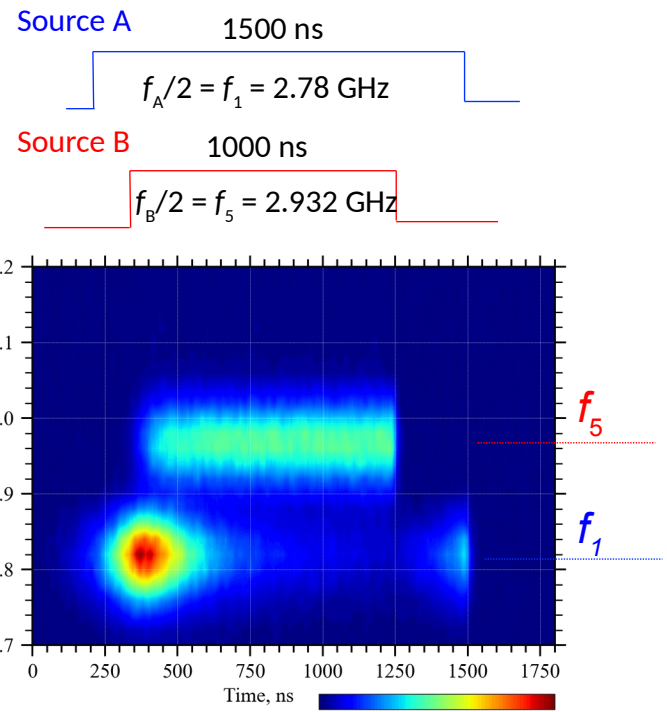

H. Merbouche et al. *Phys. Rev. Appl.* **21**, 064041 (2024)

Outline

- **Electrical techniques**
  - Broadband and cavity ferromagnetic resonance
  - Propagating spin-wave spectroscopy
  - Magneto-resistive detection of spin-waves
- **Optical techniques**
  - Time-resolved magneto-optical Kerr effect
  - Time-resolved X-ray imaging
  - Brillouin light scattering
- **Scanning probe techniques**
  - Magnetic resonance force microscopy
  - NV magnetometry

Principles of magnetic resonance force microscopy (MRFM)

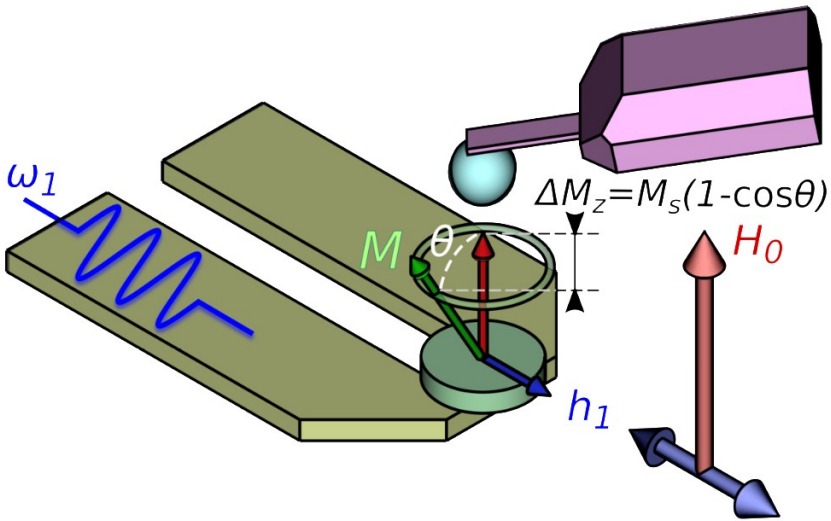

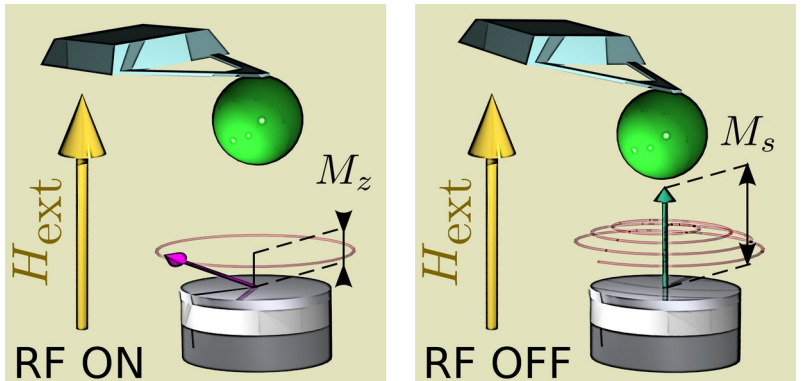

- Local, no optical access required
- Sensitive (~ 100 μ_B at 300 K)
- Detection of (static) longitudinal component of magnetization (M_z)

$$\Delta M_z = M_s - M_z = (\gamma\hbar)n_t$$

O. Klein et al. *Phys. Rev. B* **78**, 144410 (2008)

MRFM sensitivity

Limited by the thermal noise of the cantilever:

$$F_{min} = \sqrt{\frac{4k_B TkB}{\omega_c Q}}$$

→ very soft cantilever under vacuum

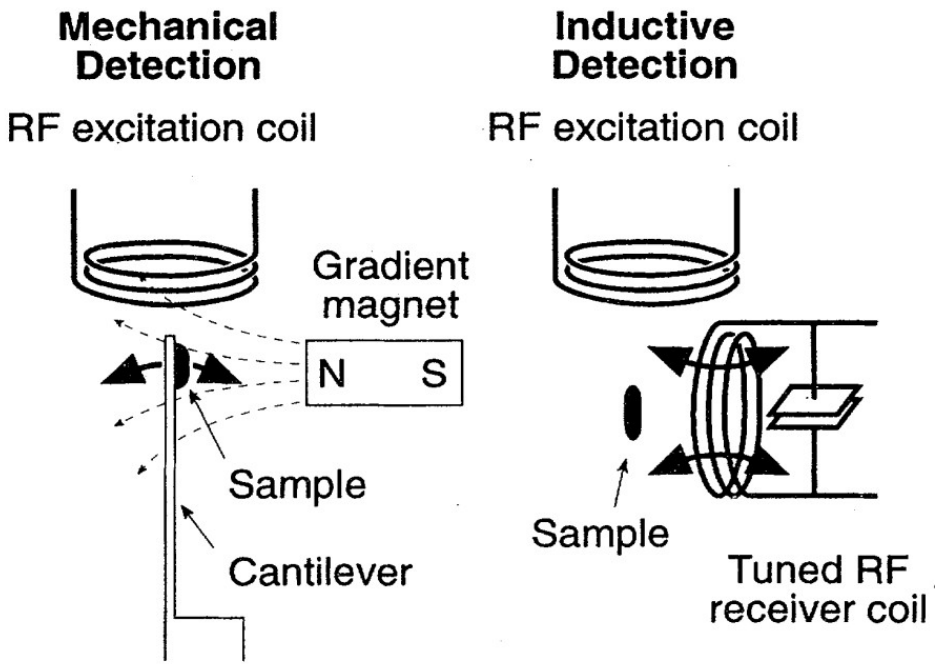

J. Sidles et al. *Rev. Mod. Phys.* **67**, 249 (1995)

Phase-lock loop tracking of the mechanical resonance

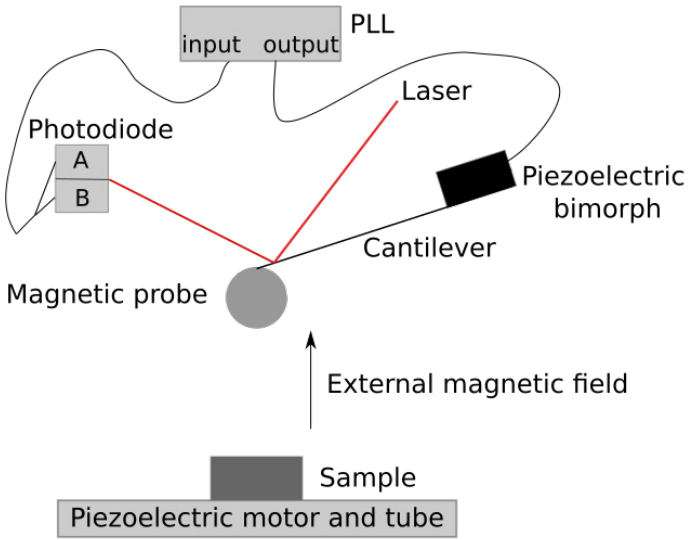

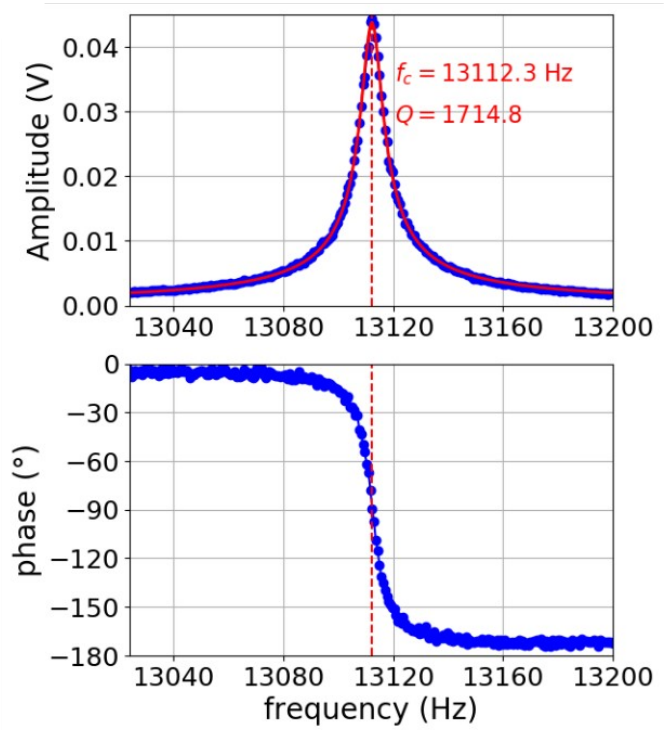

+ PID loop to maintain cantilever oscillations amplitude

FEBID grown cobalt nanospheres on ultra-soft cantilevers

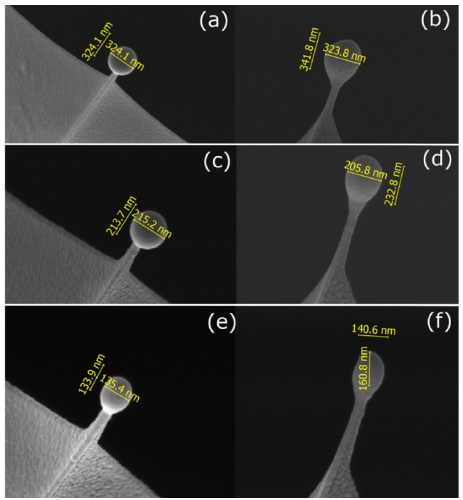

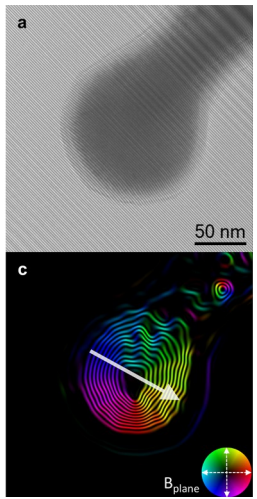

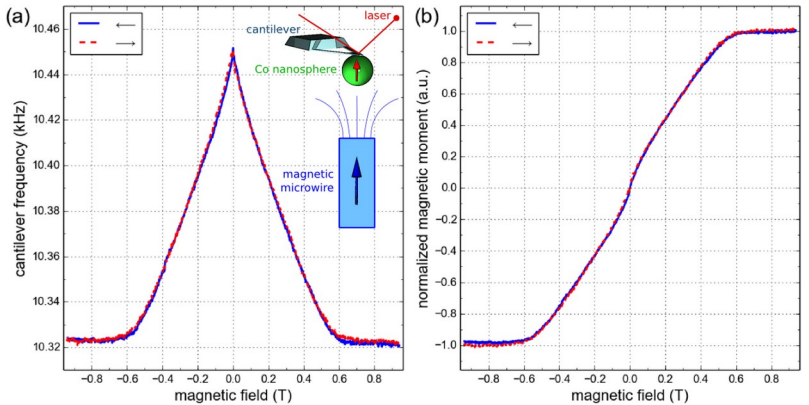

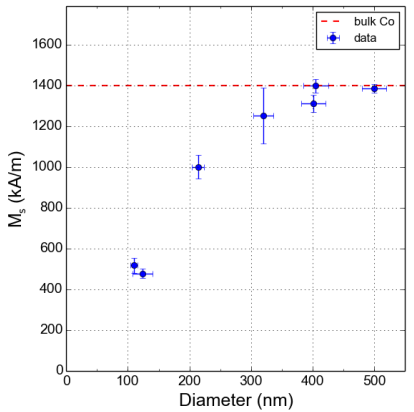

Cantilever magnetometry

$$\frac{\Delta f_c}{f_c} = -\frac{m}{2k}\left(\frac{\partial^2 B_z}{\partial z^2}\right)_{|z_0}$$

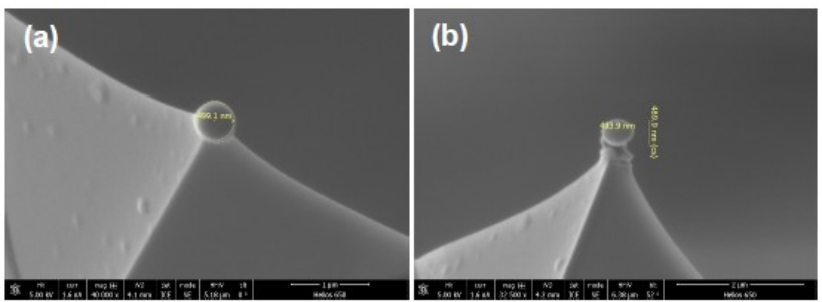

Biolever $k = 6$ mN/m; $f_c = 13$ kHz; $Q = 2000$
$D = 500$ nm, $M_s = 1050$ kA/m

S. Sangiao et al. *Beilstein J. Nanotechnol.* **8**, 2106 (2017)

MRFM signal from a single magnetic nanoparticle

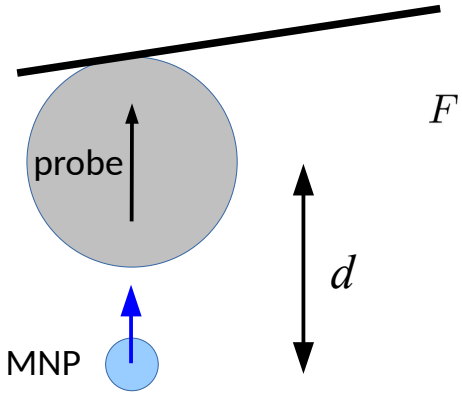

$$F = m_{\text{probe}} \times \left(\frac{\partial B_z}{\partial z}\right)_{\text{MNP}} = m_{\text{MNP}} \times \left(\frac{\partial B_z}{\partial z}\right)_{\text{probe}}$$

$$F = m_{\text{probe}} m_{\text{MNP}} \times \frac{6}{d^4}$$

MRFM signal from a single magnetic nanoparticle

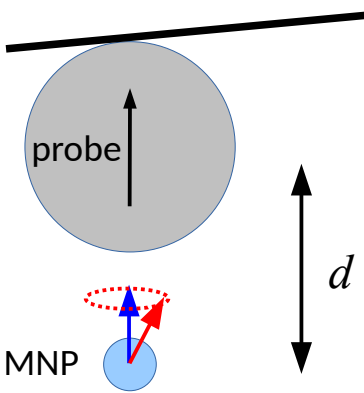

$$F = m_{\text{probe}} \times \left(\frac{\partial B_z}{\partial z}\right)_{\text{MNP}} = m_{\text{MNP}} \times \left(\frac{\partial B_z}{\partial z}\right)_{\text{probe}}$$

$$F = m_{\text{probe}} m_{\text{MNP}} \times \frac{6}{d^4}$$

$$\delta F = m_{\text{probe}} \delta m_{\text{MNP}} \times \frac{6}{d^4}$$

MNP: Iron oxide particle, *M* = 350 kA/m, Ø = 20 nm
Probe: Co nanospere, *M* = 1200 kA/m, Ø = 100 nm
Probe-MNP separation: *d* = 100 nm

$$\frac{\delta m}{m} = 10^{-3} \Longrightarrow \theta \simeq 2.5^{\circ}$$

m_{MNP}	$(B_z)_{\text{probe}}$	$\left(\frac{\partial B_z}{\partial z}\right)_{\text{probe}}$	F	δF
1.5 10^{-18} J/T	125 mT	3.8 10^{6} T/m	5.5 pN	5.5 fN ~ 8 F_{min} (1 Hz bandwidth)
1.6 10^{5} μ_B		F_{min} ≡ reversal of 10 spins in the MNP		

MRFM spin-wave spectroscopy of YIG nanodisks

PLD grown **YIG 20 nm**
α = 4 x 10^{-4}

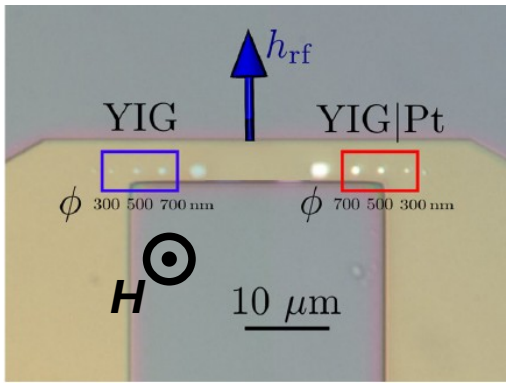

Out-of plane geometry (*H* = *5* kOe)

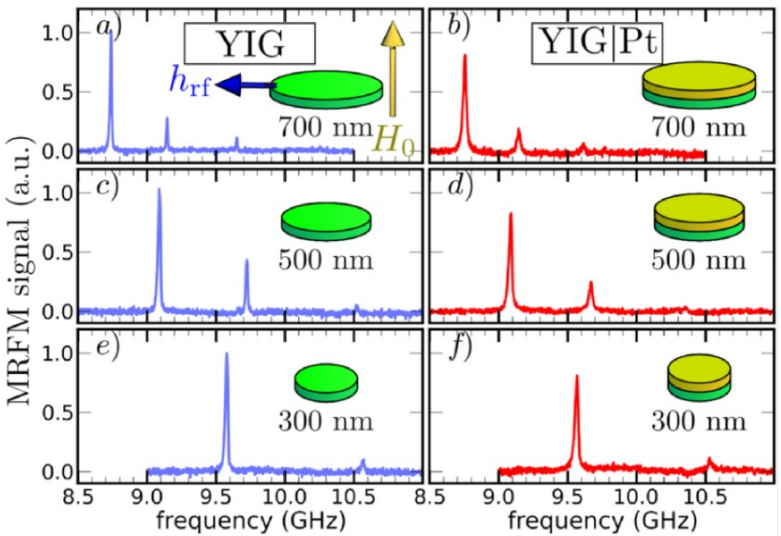

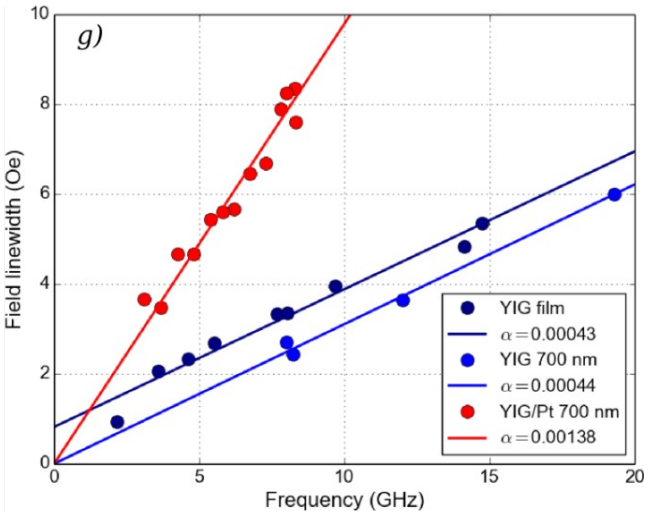

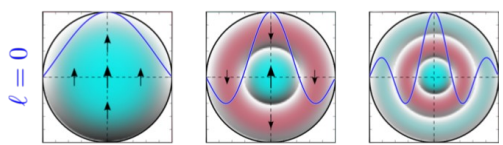

- discretization of SW modes
- increased damping: spin pumping at YIG/Pt interface

C. Hahn et al. *Appl. Phys. Lett.* **104**, 152410 (2014)

Spin-wave spectroscopy in the vortex cone state

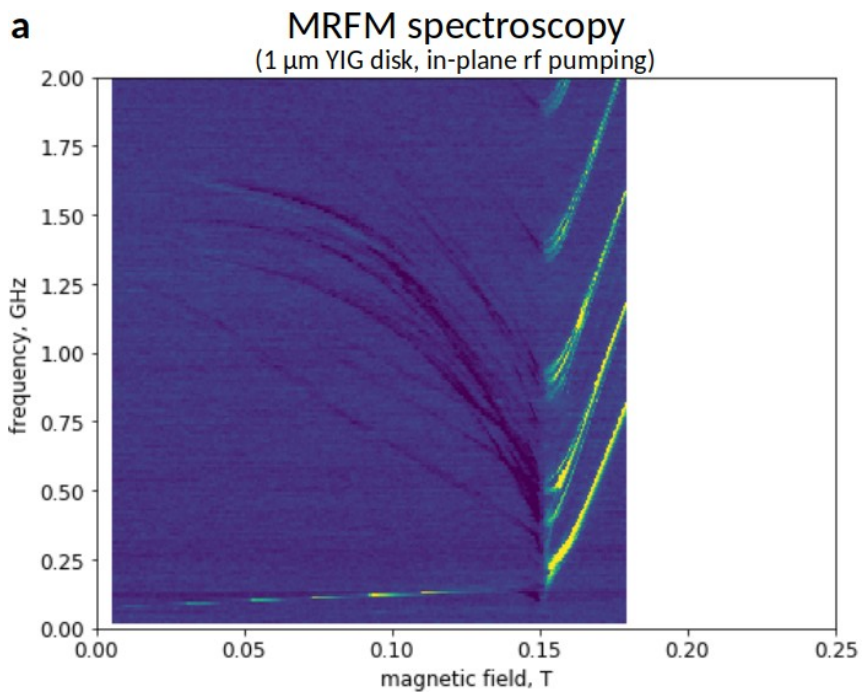

V. Castel et al. *Phys. Rev. B* **85**, 184419 (2012)
B. Taurel et al. *Phys. Rev. B* **93**, 184427 (2016)

Spin-wave spectroscopy of a spin-torque nano-oscillator

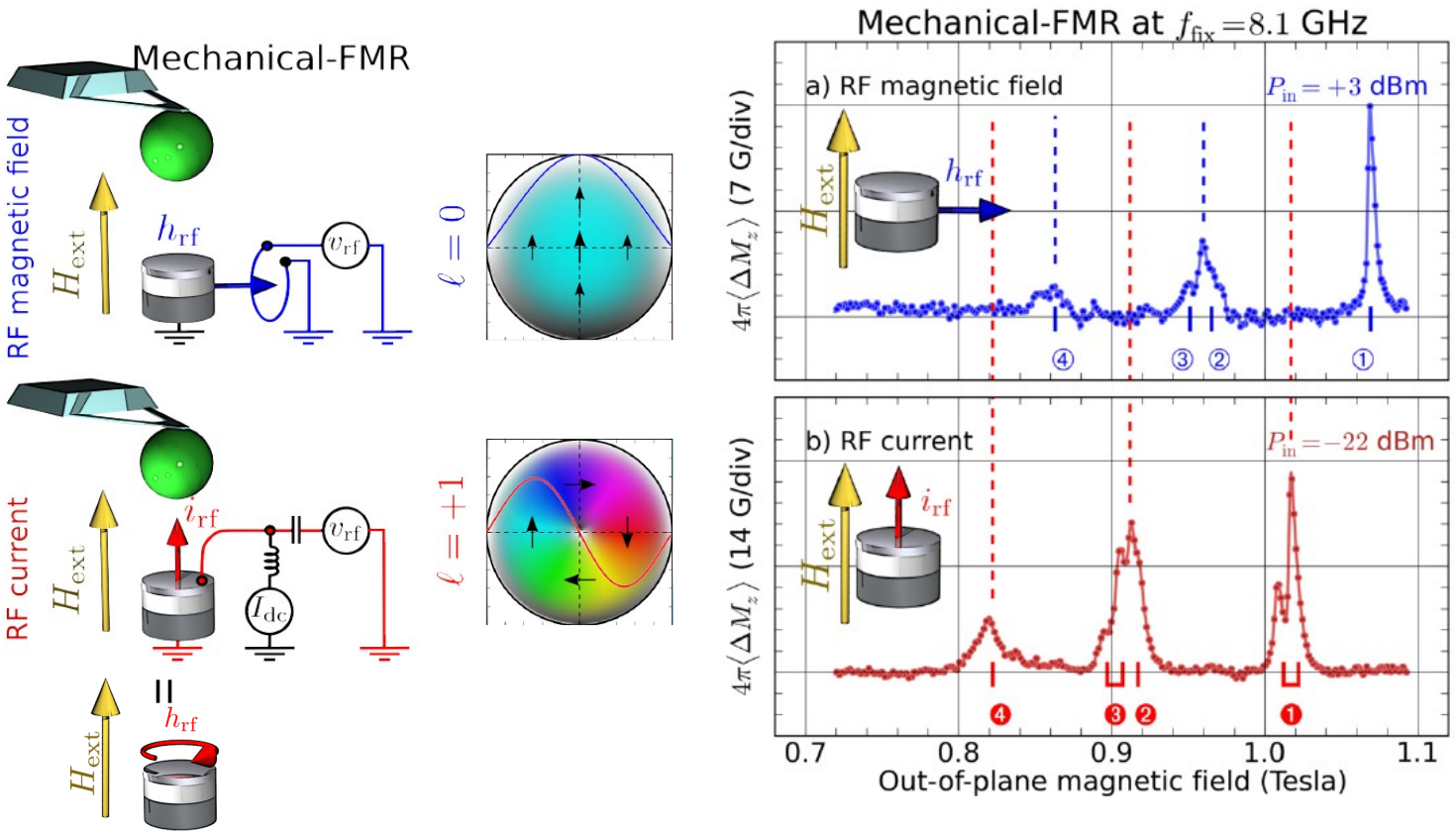

Different pumping symmetries → different spin-wave modes excited

V. Naletov et al. *Phys. Rev. B* **84**, 224423 (2011)

MRFM imaging: mode mapping in confined structures

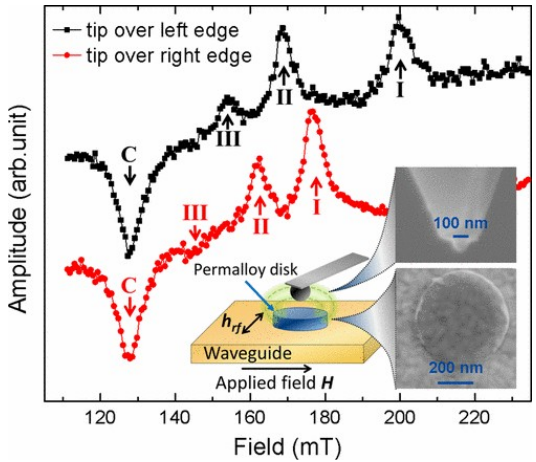

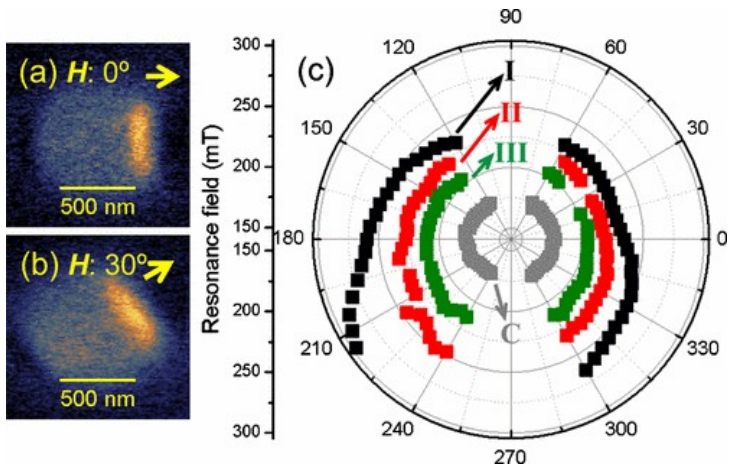

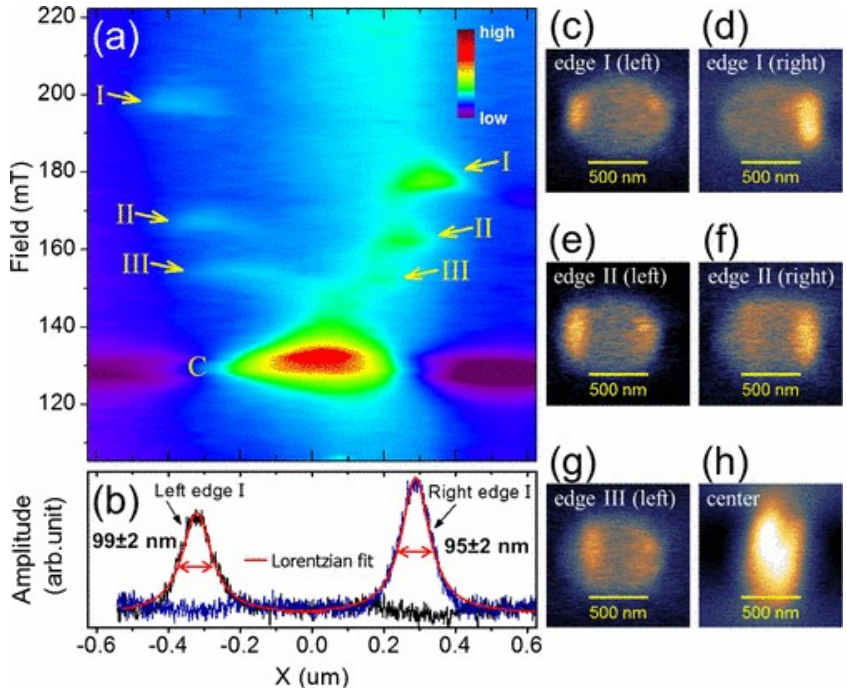

F. Guo, et al. *Phys. Rev. Lett.* **110**, 017601 (2013)

MRFM imaging: mode localization in extended films

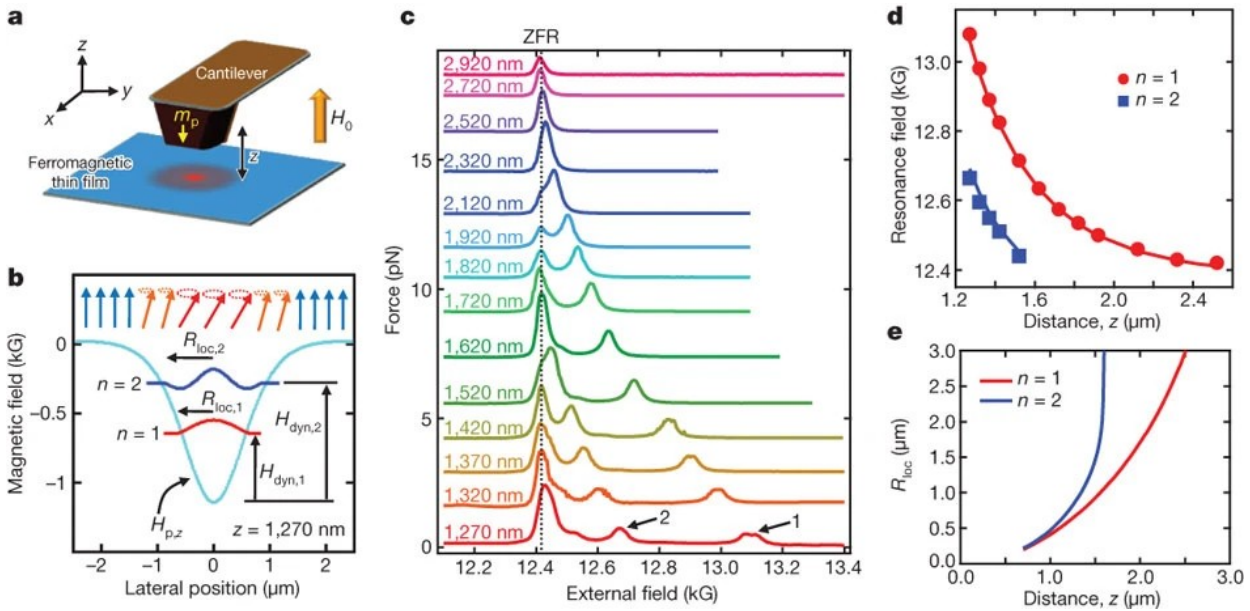

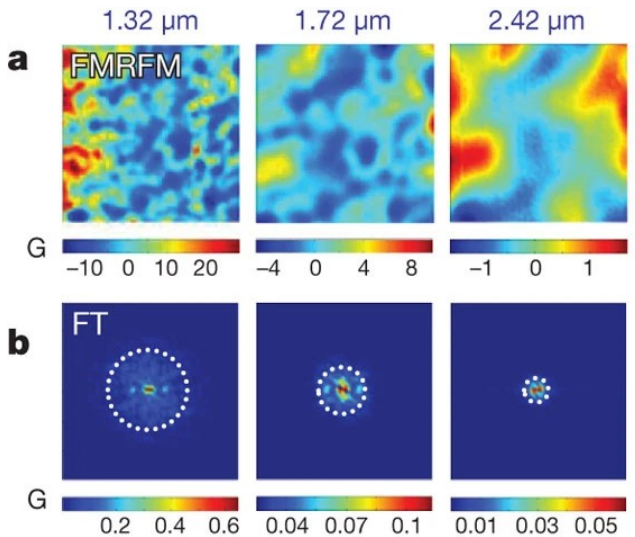

I. Lee et al. *Nature* **466**, 845-848 (2010)

Nanoscale imaging of damping in extended films

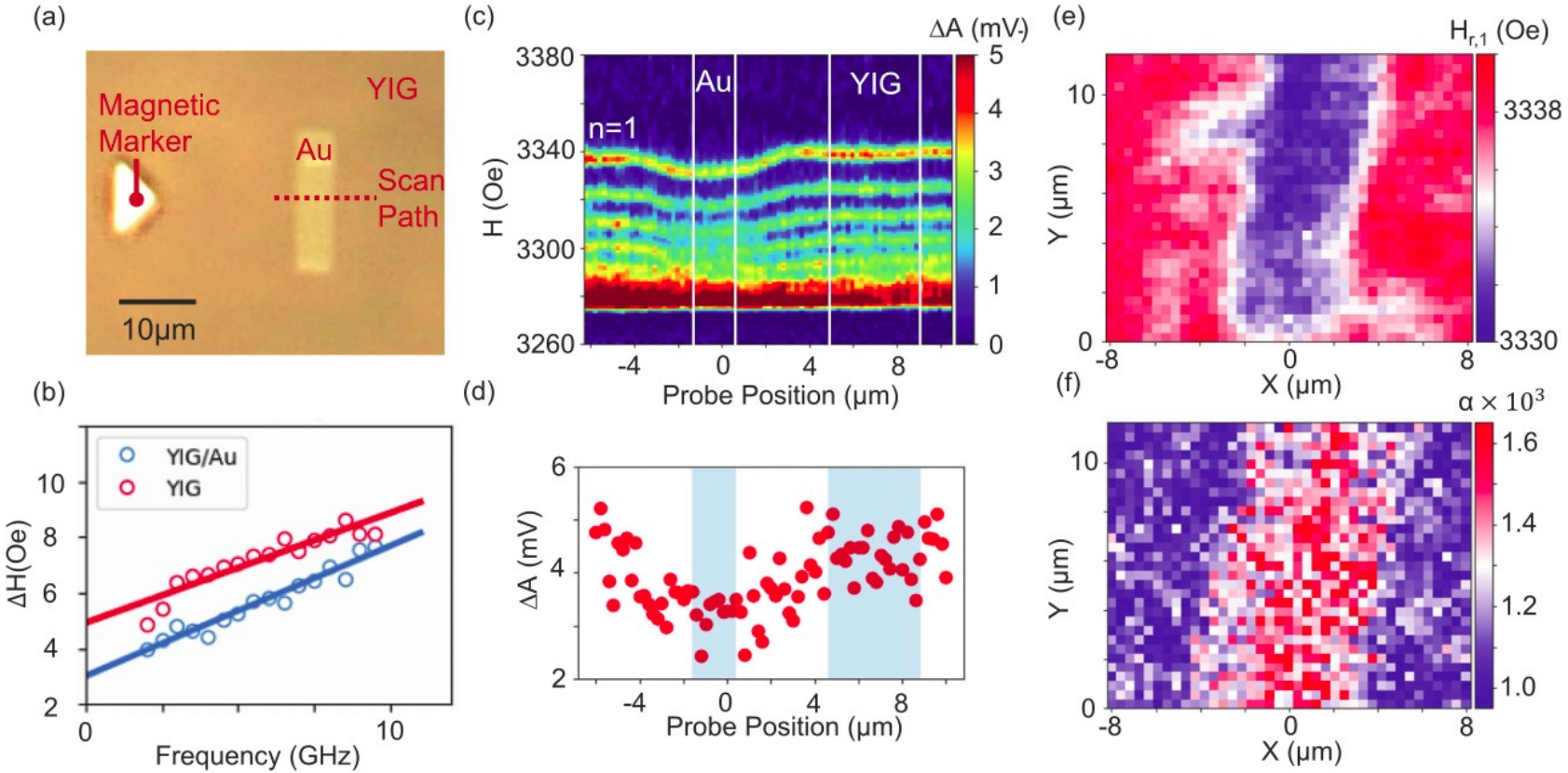

G. Wu et al. *Appl. Phys. Lett.* **118**, 042403 (2021)

Outline

- **Electrical techniques**
  - Broadband and cavity ferromagnetic resonance
  - Propagating spin-wave spectroscopy
  - Magneto-resistive detection of spin-waves
- **Optical techniques**
  - Time-resolved magneto-optical Kerr effect
  - Time-resolved X-ray imaging
  - Brillouin light scattering
- **Scanning probe techniques**
  - Magnetic resonance force microscopy
  - NV magnetometry

Nitrogen-Vacancy (NV) center in diamond: a magnetic field sensor

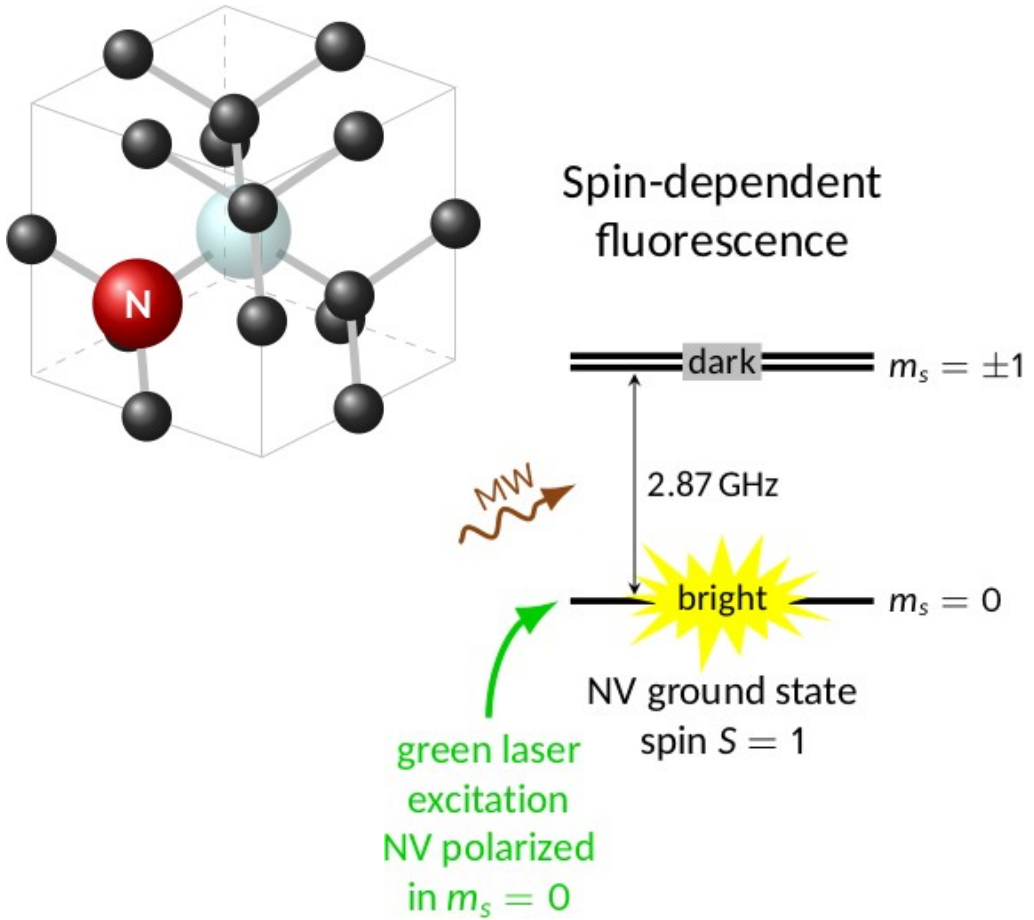

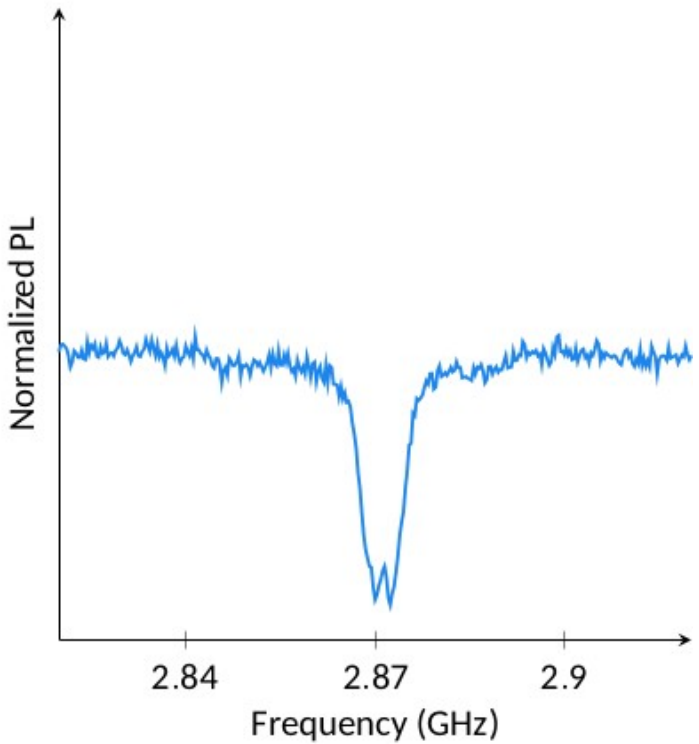

L Rondin et al. *Rep. Prog. Phys.* **77**, 056503 (2014)

Nitrogen-Vacancy (NV) center in diamond: a magnetic field sensor

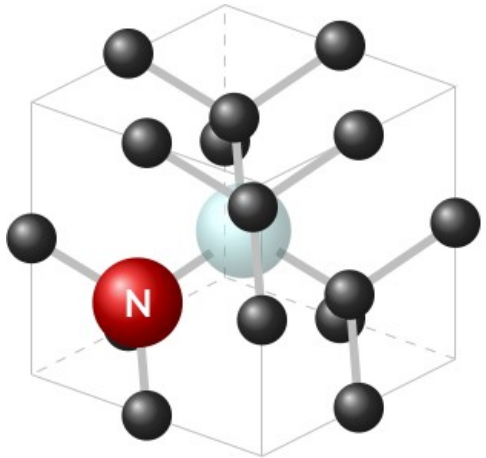

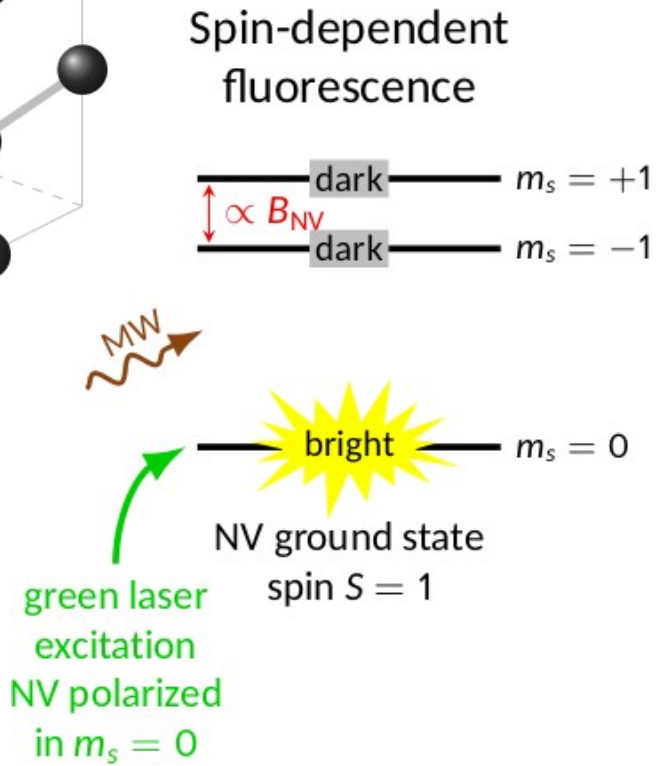

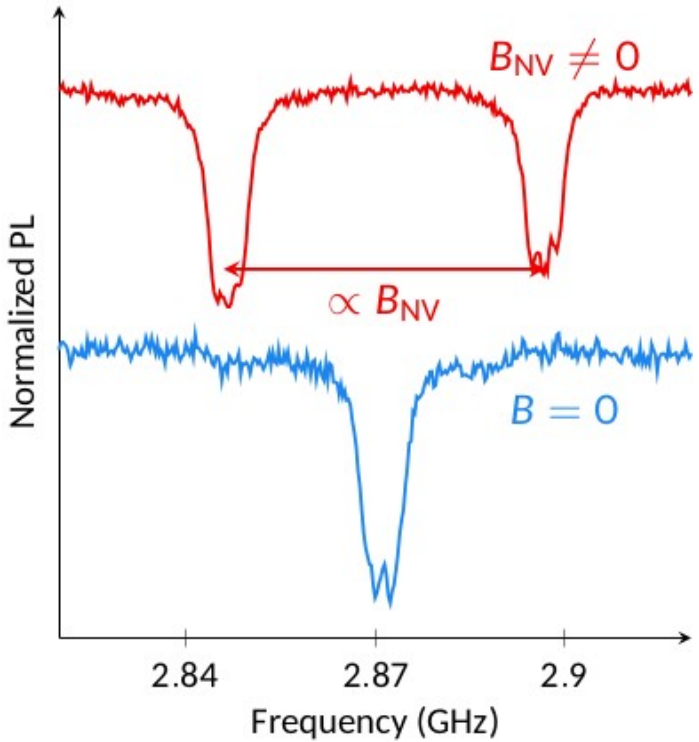

L Rondin et al. *Rep. Prog. Phys.* **77**, 056503 (2014)

Quantum sensing with a NV center

$$\mathcal{H}_{gs} = h\left[D_{NV}\hat{S}_z^2 + \gamma_{NV}\hat{\vec{S}}\cdot\vec{B}\right] \quad \text{with} \quad \begin{cases} D_{NV} \simeq 2.87\,\text{GHz} \\ \gamma_{NV} \simeq 28\,\text{GHz}\,\text{T}^{-1} \end{cases}$$

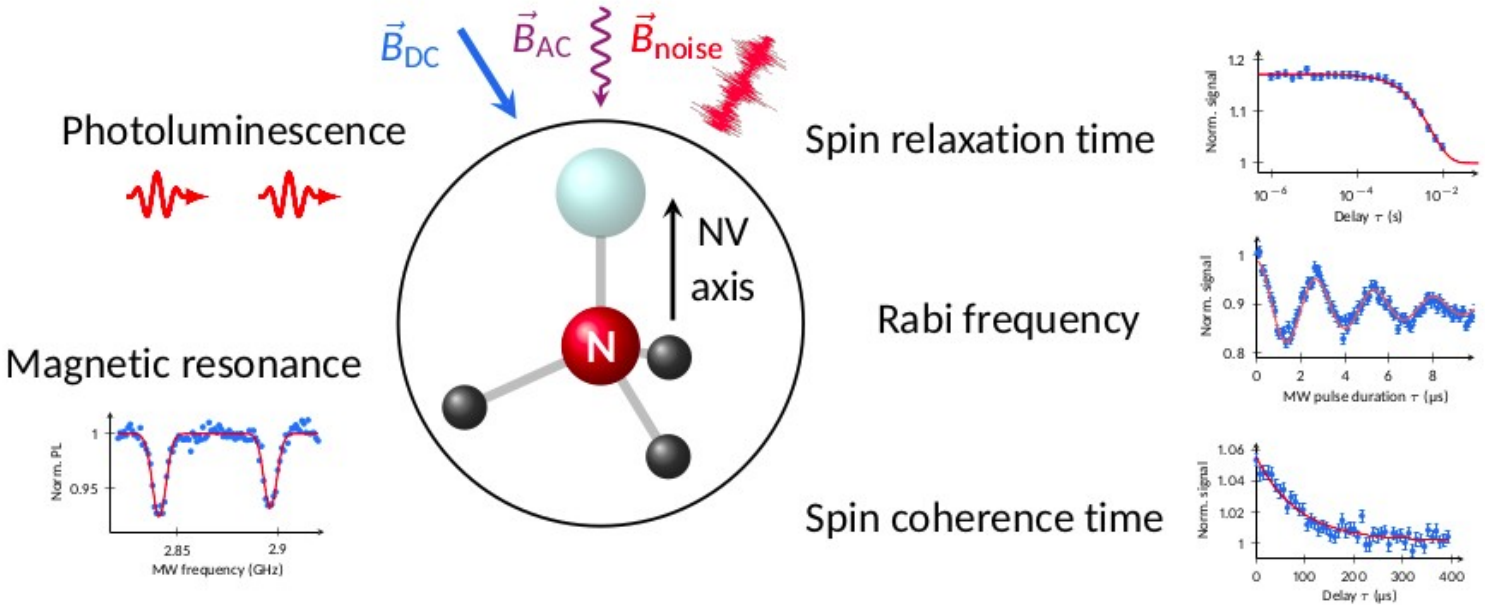

Highly sensitivite, non perturbative, quantitative, nanoscale spatial resolution

Imaging with NV center(s)

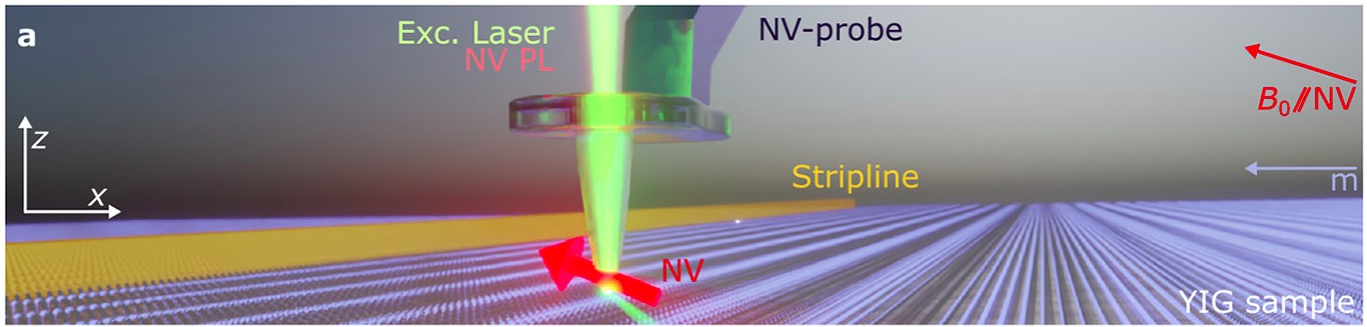

First approach: scanning a tip with a single NV center at its apex

Second approach: scanning the laser spot on an ensemble of NV centers

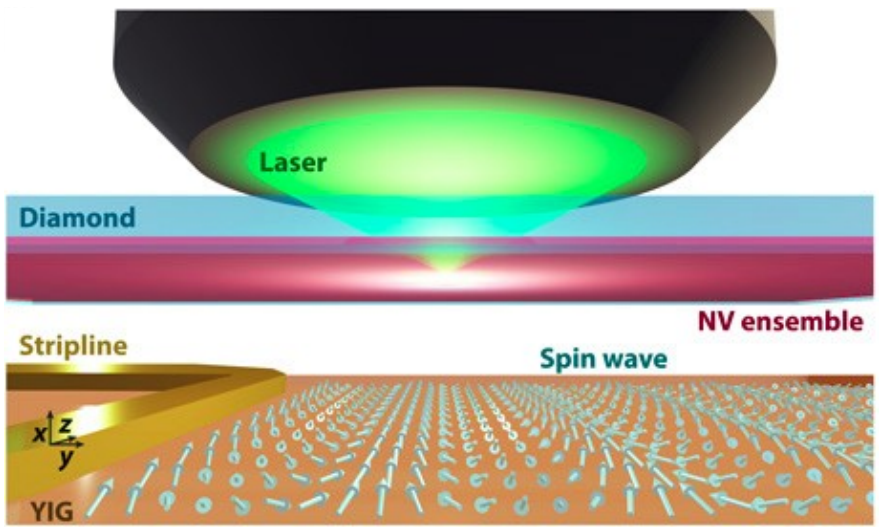

B. G. Simon et al. *Nano Lett.* **22**, 9198 (2022)

I. Bertelli, Science Adv. **6**, eabd3556 (2020)

Detecting the rf strayfield of spin-waves with a NV center

NV – sample distance

SW spatial profile: $\mathbf{m}_\perp(y) = m_\perp^0 \mathrm{Re}\{e^{i(k_y y-\omega t)}(\hat{\mathbf{y}} - i\eta\hat{\mathbf{x}})\}$

$\rightarrow \mathbf{B}_{SW}(y) = -B_{SW}^0 \mathrm{Re}\{e^{i(k_y y-\omega t)}(\hat{\mathbf{y}} + i\,\mathrm{sgn}(k_y)\,\hat{\mathbf{x}})\}$ with $B_{SW}^0 = \mu_0 m_\perp^0 (1 + \mathrm{sgn}(k_y)\eta)\,|\mathbf{k}|\,d\,e^{-|k_y|x_0}/2$

$\rightarrow \omega_{Rabi}(y) = \sqrt{2}\,\gamma\,|B_{SW}^0 \cos^2\left(\frac{\phi}{2}\right) e^{ik_y y} - B_{REF}|$

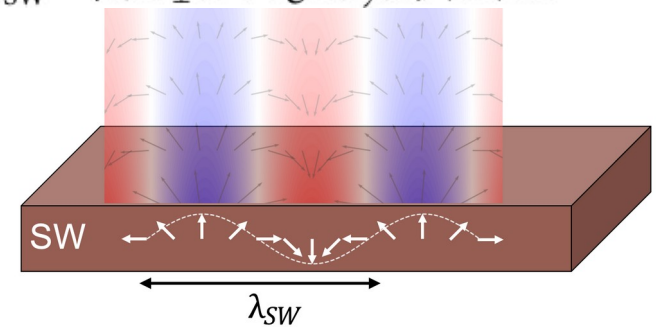

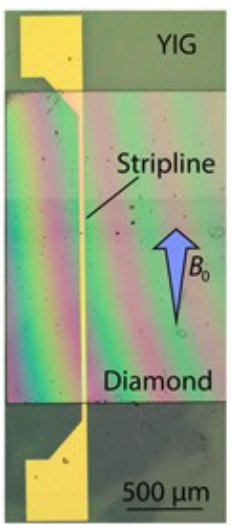

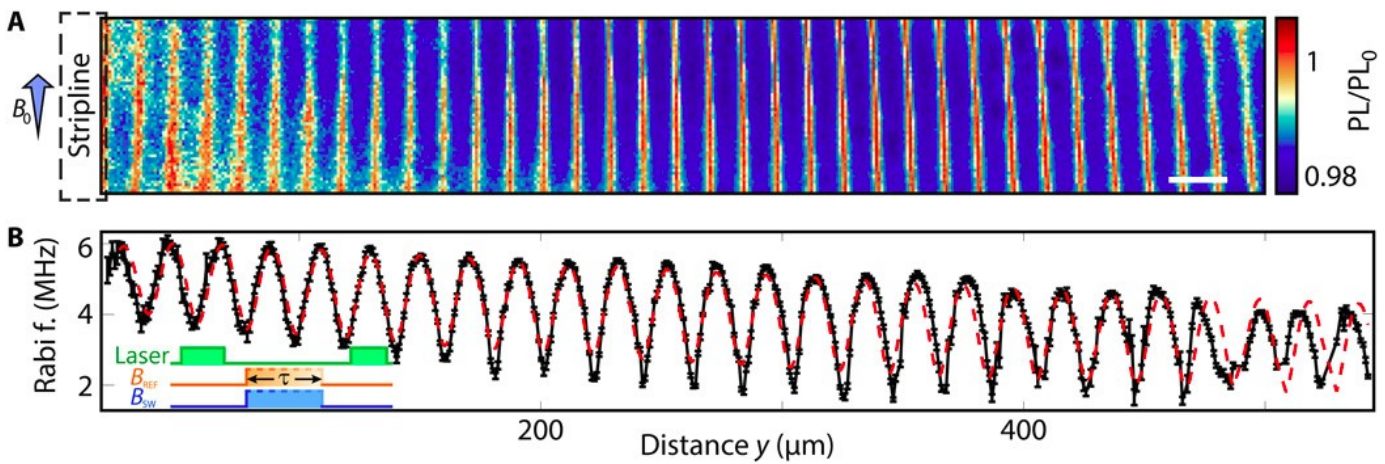

I. Bertelli, Science Adv. **6**, eabd3556 (2020)

Filtering the spin-wave wavevector with the NV – sample distance

$$B_{SW} \propto f_k - ke^{-kd}$$

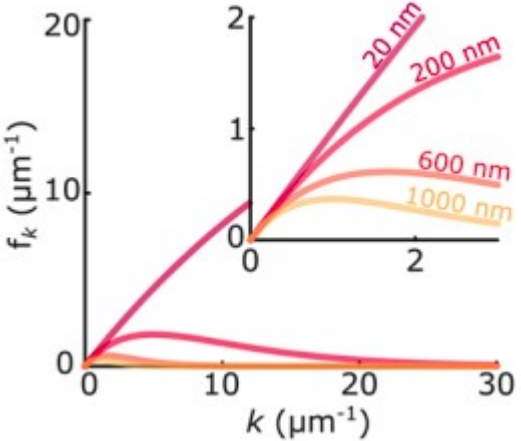

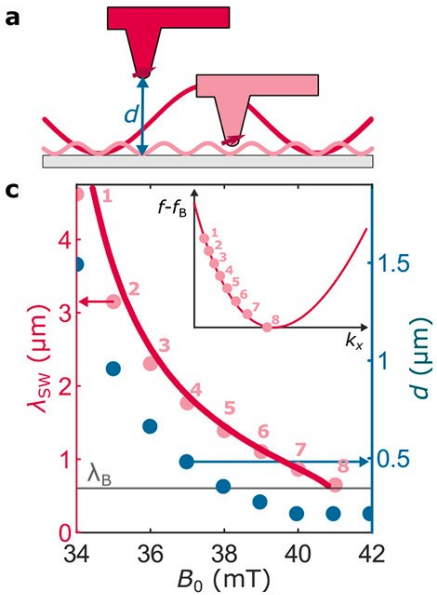

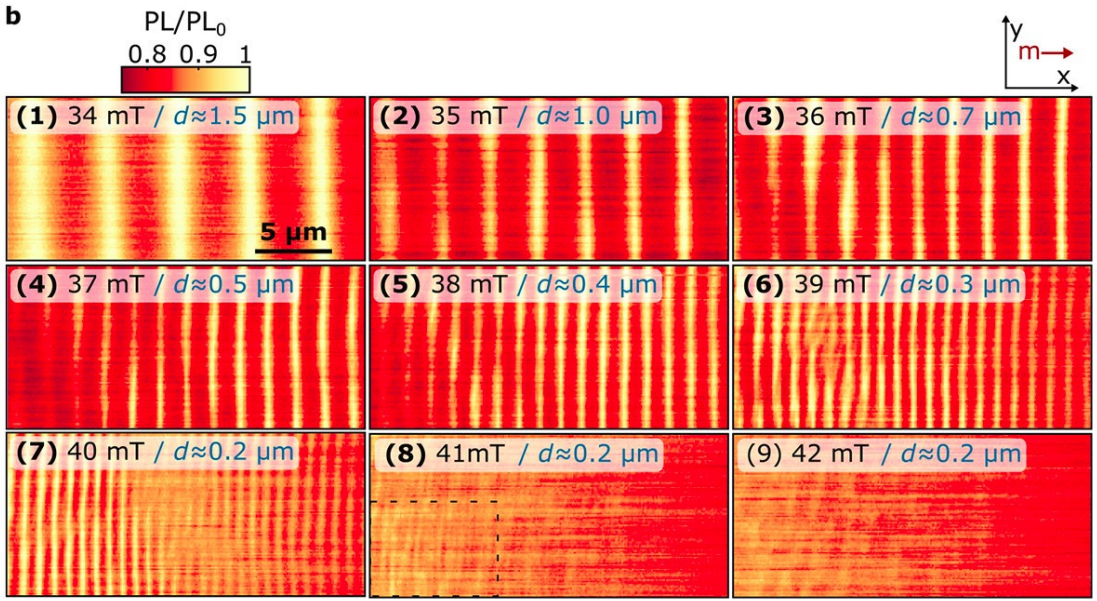

B. G. Simon, *Nano Lett.* **22**, 9198 (2022)

Measuring magnetic noise with NV relaxometry

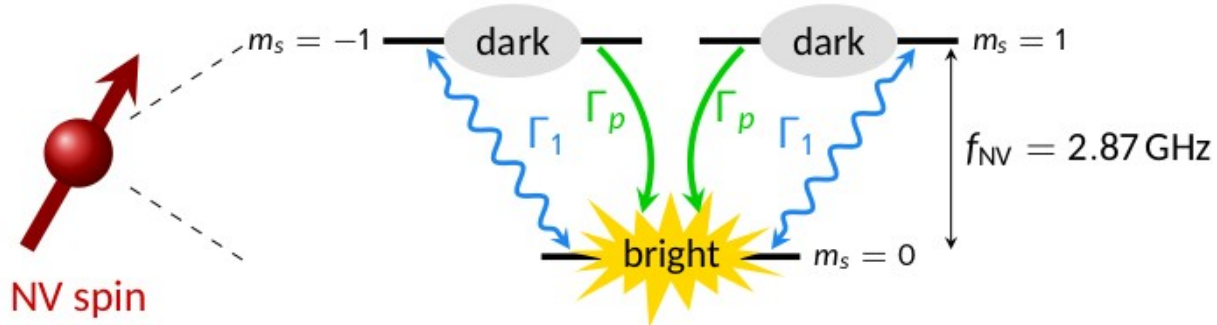

Relaxation rate $\Gamma_1 \propto S_{B_\perp}(f_{NV})$ magnetic field spectral density at the resonance frequency f_{NV}

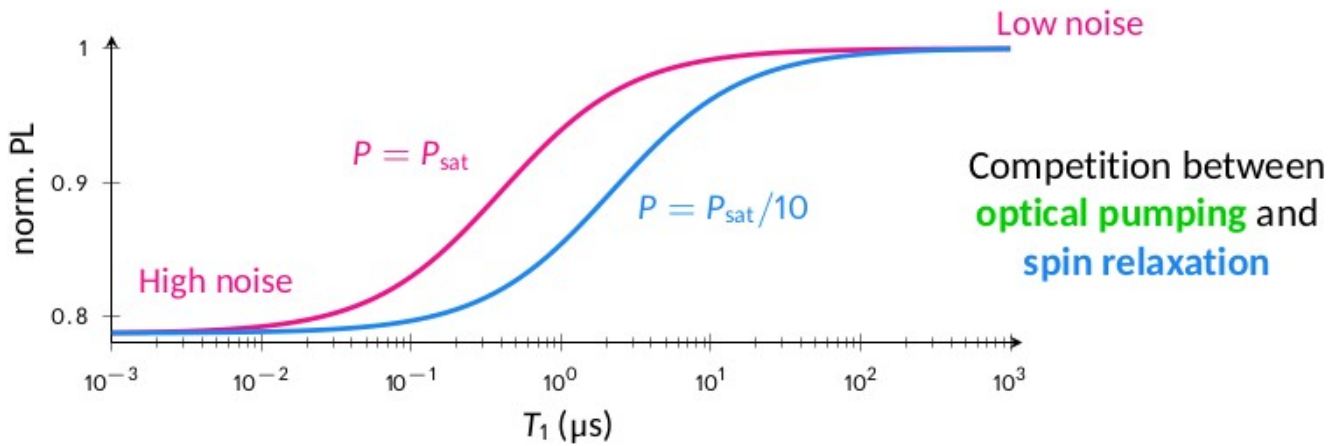

M. Rollo et al. *Phys. Rev. B* **103**, 235418 (2021)

Thermal spin waves confined in domain walls

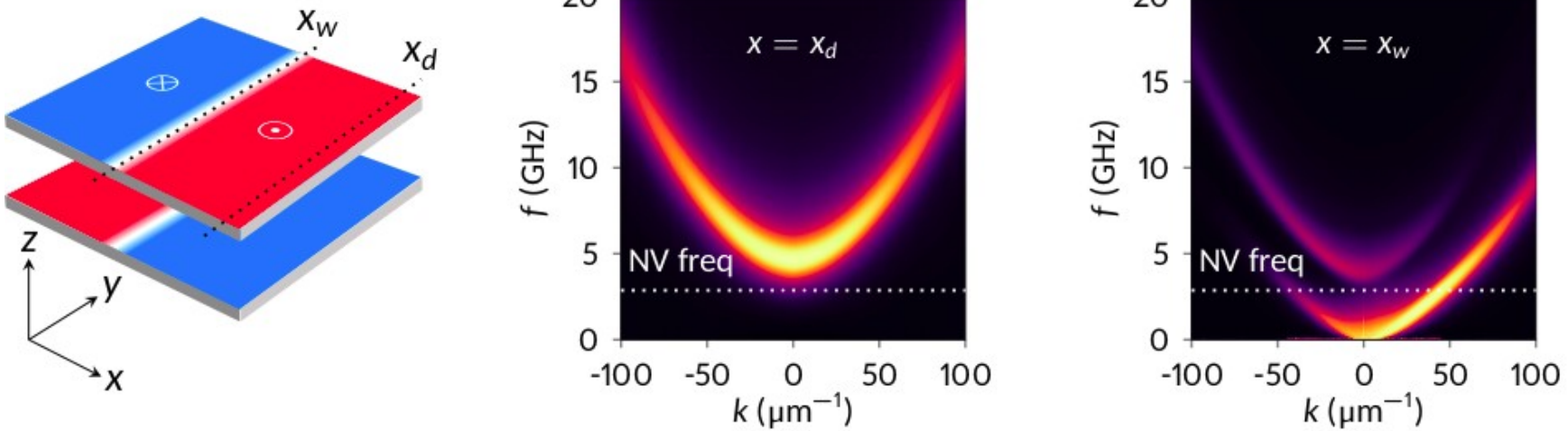

- NV frequency slightly below the gap, in the tail of power spectral density, which is the reason why we detect some noise when approaching the tip.
- No gap in the domain walls, presence of modes at the NV frequency: **the NV center is more sensitive to the noise from the walls!**

A. Finco et al. *Nat. Commun.* **12**, 767 (2021)

Thermal spin waves confined in domain walls

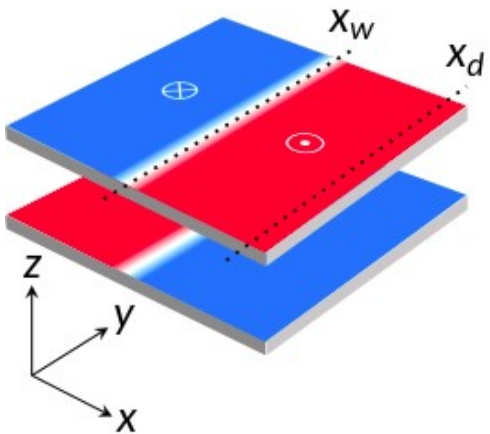

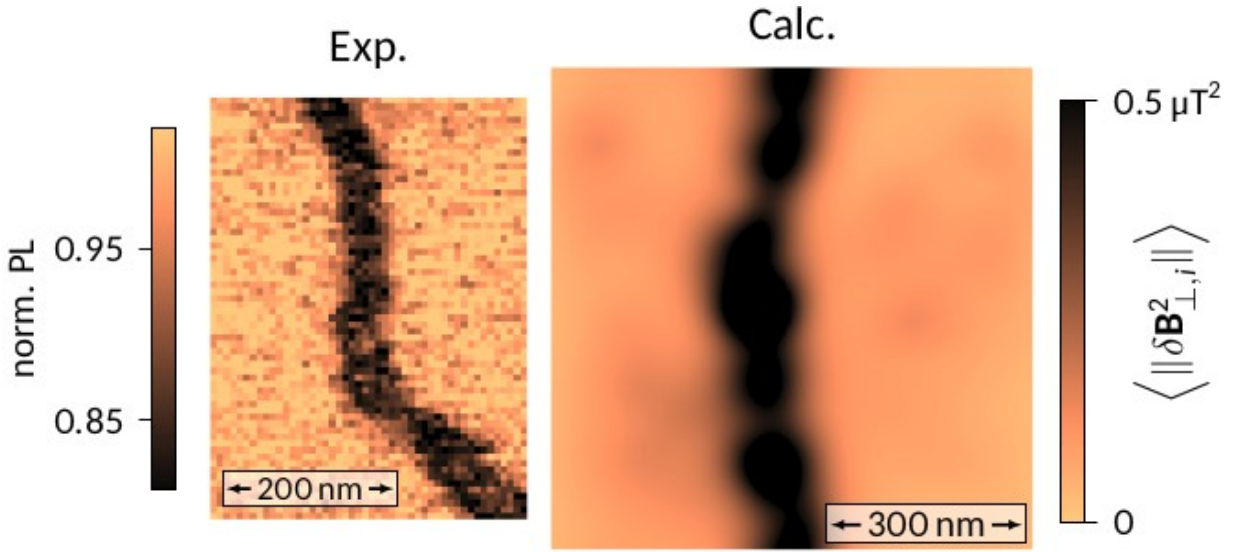

- NV frequency slightly below the gap, in the tail of power spectral density, which is the reason why we detect some noise when approaching the tip.
- No gap in the domain walls, presence of modes at the NV frequency: **the NV center is more sensitive to the noise from the walls!**

A. Finco et al. *Nat. Commun.* **12**, 767 (2021)

Remarkable features

- **Electrical techniques – easy implementation, close to applications**
  - Broadband and cavity ferromagnetic resonance – characterization of ultra-thin films
  - Propagating spin-wave spectroscopy – scalability, access to spin-wave dispersion
  - Magneto-resistive detection of spin-waves – highly sensitive, small volumes
- **Optical techniques – high temporal resolution, diffraction limited**
  - Time-resolved magneto-optical Kerr effect – phase sensitive, ~ 250 nm resolution
  - Time-resolved X-ray imaging – element specific, ~ 20 nm resolution
  - Brillouin light scattering – highly sensitive, spectral resolution, ~ 250 nm resolution
- **Scanning probe techniques – versatile, ~50 nm resolution, quantitative**
  - Magnetic resonance force microscopy – broad field & frequency range
  - NV magnetometry – highly sensitive, non perturbative

Useful references to prepare this lecture (one per technique)

1. *Implementation of field-differential phase-resolved microwave magnetic spectroscopy*, W. Legrand, Rev. Sci. Instrum. **96**, 034708 (2025)

2. *Propagating-spin-wave spectroscopy using inductive antennas: Conditions for unidirectional energy flow*, T. Devolder, Phys. Rev. Appl. **20**, 054057 (2023)

3. *Comparative measurements of inverse spin Hall effects and magnetoresistance in YIG/Pt and YIG/Ta*, C. Hahn et al. Phys. Rev. B **87**, 174417 (2013)

4. *Time-Resolved Kerr Microscopy of Spin Waves Propagating in Magnetic Nanostructures*, H. S. Körner, PhD thesis, Universität Regensburg (2017)

5. *Time-resolved x-ray imaging of nanoscale spin-wave dynamics at multi-GHz frequencies using low-alpha synchrotron operation*, S. Mayr et al. Appl. Phys. Rev. **11**, 041411 (2024)

6. *Micro-focused Brillouin light scattering: imaging spin waves at the nanoscale*, T. Sebastian et al. Frontiers in Physics **3**, 35 (2015)

7. *Ferromagnetic resonance force spectroscopy of individual submicron-size samples*, O. Klein et al. Phys. Rev. B **78**, 144410 (2008)

8. *Single spin magnetometry and relaxometry applied to antiferromagnetic materials*, A. Finco & V. Jacques, APL Mater. **11**, 100901 (2023)

Acknowledgements (kind people providing slides out of friendship)

Gaël Thiancourt + Thibaut Devolder (PSWS), Jean-Paul Adam (µ-BLS)

André Thiaville (BLS)

Jean-Yves Chauleau (TR-MOKE), Hugo Merbouche (µ-BLS)

Aurore Finco (NV magnetometry)